

# Bridge health monitoring in the United States: A review

Piervincenzo Rizzo\*<sup>1</sup> and Alireza Enshaeian<sup>2a</sup>

<sup>1</sup> Department of Civil and Environmental Engineering, University of Pittsburgh, Pittsburgh, PA 15261, USA

<sup>2</sup> Laboratory for Nondestructive Evaluation and Structural Health Monitoring Studies,  
Department of Civil and Environmental Engineering, University of Pittsburgh, Pittsburgh, PA 15261, USA

(Received August 5, 2020, Revised October 30, 2020, Accepted November 12, 2020)

**Abstract.** The assessment of bridges' health has become a relevant component of the maintenance paradigm especially in those countries in which many structures are rated in poor condition and/or are over 50 years old. Additionally, the permanent monitoring of bridges helps engineers in validating the design prediction of bridge structural response to external loads. With more than 600,000 highway bridges, 46.4% of which rated as fair and 7.6% rated in poor condition, United States is one of those countries in which the installation of reliable bridge health monitoring systems is strategically necessary to minimize and optimize repair and rehabilitation costs and to minimize the risk of failures. In this paper, a thorough review of the scientific literature on structural health monitoring systems installed in U.S. bridges over the last 20 years is presented. This review aims to offer interested readers a holistic perspective of recent and current state-of-the-art bridge health monitoring systems and to extract a "general paradigm" that is common to many real structures. The review, conducted through a comprehensive search of peer-reviewed documents available in the scientific literature, discusses more than sixty bridges in terms of the instrumentation used, scope of the monitoring, and main outcomes. Overall, it was found that the monitoring systems provide a valuable tool to compare the structural responses predicted using analytical or numerical tools with the real response of the given structures. Owing to the relative short time span of the monitoring period, most of the monitoring systems did not flag any serious structural flaws that required the closure of the bridge monitored.

**Keywords:** structural health monitoring; bridges; state-of-the-art review; United States

---

## 1. Introduction

In the United States (U.S.) and in other parts of the world, some civil infrastructures are either in poor condition, are operating beyond their designed life, and/or are subjected to harsh natural events such as extreme winds and earthquakes. Additionally, the growth of the world population increases the tonnage of commodities and the volume of vehicular and public transportation traffic moved daily. Finally, some infrastructures may incorporate novel materials whose degradation processes are not well known and failures may occur even shortly after inaugurations. According to the U.S. Federal Highway Administration (FHWA) (FHWA 2019a), there are over 600,000

---

\*Corresponding author, Professor, E-mail: [pir3@pitt.edu](mailto:pir3@pitt.edu)

<sup>a</sup> Ph.D. Student, E-mail: [ale69@pitt.edu](mailto:ale69@pitt.edu)

(616,096) highway bridges<sup>1</sup> in the United States. Of these, about 46% are rated in good condition, 46.4% are rated as fair, and the remaining 7.6% are rated in poor<sup>2</sup> condition (Federal Highway Administration 2019c). Other statistics identified 54,259 bridges as “structurally deficient<sup>3</sup>” (Virginia Department of Transportation 2019). In the U.S., the evaluation of bridges starts with a periodic inspection (at least every two years), conducted in accordance with the National Bridge Inspection Standards, to determine the current condition. When a given bridge shows problematic areas, it may be inspected more frequently at the discretion of the owner. Any structure with a span longer than 6 m is rated on a scale 0 to 9 for National Bridge Inventory (NBI). A rate of 9 indicates a new bridge whereas a rate of 0 identifies bridges being out of service. A structurally poor bridge is rated 4 or less for superstructure, deck and/or substructure (Ahlborn *et al.* 2010).

As traditional nondestructive evaluation (NDE) maintenance can do little when flaws start or become critical between two inspections, there is a growing interest in cost-effective structural health monitoring (SHM) strategies to monitor bridges 24/7. SHM is the scientific process of identifying damage non-destructively using a network of sensors. SHM evolves the maintenance paradigm from “time-based” NDE in which a structure is inspected periodically, to permanent-based where sensors monitor 24/7 to flag, locate, and quantify damage as it happens. The sensors measure physical characteristics like strain, acceleration, temperature, just to mention a few, while dedicated hardware/software elaborates the set of time series streamed from the sensors.

In this paper, the results of a thorough review of current and past SHM instrumentation installed in U.S. bridges in the last 20 years is presented. The information considered for inclusion is based on peer-reviewed documents and/or technical reports available in the scientific literature. The motivation behind this review article is multi-fold: to provide the broadest possible knowledge about bridge SHM in the U.S.; to emphasize the escalating efforts over the last decade; to identify possible roadblocks that prevents further expansion of SHM strategies to a virtual unlimited number of bridges. Owing to the vast information found during this study, interested readers are referred to the bibliography given to gain insights about individual programs. Whenever possible, and compatible to the amount of information found, this paper includes a discussion on data management, analysis, and inference approaches to assess reliable safety evaluation, resilience assessment and future life prediction of bridges. The following databases were used beginning January 2020: TRID database, Google Scholar, and Scopus. Queries like: “structural health monitoring” AND “bridges” AND “United States” were performed. Inclusion criteria were peer-review articles, technical reports submitted to U.S. Federal Agencies and Departments of Transportation. Primary exclusion criteria were patents, conference proceedings abstracts, advertisement material. Secondary exclusion criteria were short communications, conference papers, and websites, for which however a few exceptions were made in absence of other documentation. Other criteria of exclusions were all those methodologies related with remote

---

<sup>1</sup> **Highway Bridge:** A public vehicular structure more than 6.1 meters (20 feet) in length that spans an obstruction or depression. In data terms, all of the following apply: Item 5a=1; Item 49>=6.1 meters; Item 112=Y; and Item 42a=1 or 4 or 5 or 6 or 7 or 8 (Federal Highway Administration, (2019b)).

<sup>2</sup> **Good (G), Fair (F), Poor(P):** These terms are defined in accordance with the [Pavement and Bridge Condition Performance Measures final rule](#), published in January of 2017. Bridge Condition is determined by the lowest rating of National Bridge Inventory (NBI) condition ratings for Item 58 (Deck), Item 59 (Superstructure), Item 60 (Substructure), or Item 62 (Culvert). If the lowest rating is greater than or equal to 7, the bridge is classified as Good; if it is less than or equal to 4, the classification is Poor. Bridges rated 5 or 6 are classified as Fair (Federal Highway Administration 2019b).

<sup>3</sup> A “structurally deficient” bridge is a structure in which there are elements “*that need to be monitored and/or repaired*.” The fact that a bridge is “structurally deficient” does not imply that it is likely to collapse or that it is unsafe. It means the bridge must be monitored, inspected and maintained” (Virginia Department of Transportation 2019)

sensing such as unmanned aerial vehicles, video-based (e.g., Khuc and Catbas 2018). and infrared-based cameras use, GPS, etc...Finally, scour monitoring was not included and the interested readers are referred to Hunt (2009) for an interesting review.

This paper is structured as follows. Section 2 provides an overall account of SHM paradigms and their implementation in bridges. Section 3 presents two lists of bridges instrumented with SHM systems: the first list was adapted from Xu and Xia (2011); the second list was compiled in this study. Section 4 describes the instrumentation programs of the bridges listed in Section 3. For each structure, a synopsis of the instrumentation is given along with the scope and, where available, some main outcomes. Owing to the amount of signal processing, data analysis, reliability models, etc... a detailed account of each and every analysis could not be provided. Section 5 ends this review with some concluding remarks.

## 2. Structural health monitoring

SHM can be defined as the process of using continuous information obtained from an array of sensors deployed in a structural system, to infer in near real-time its structural integrity (damage diagnosis) and estimate its remaining useful life (damage prognosis) (Farrar and Worden 2007, 2012, Adams 2007, Karbhari and Ansari 2009, Yan *et al.* 2017). SHM systems may be complemented by structural analysis and/or finite element models (FEMs) that enable a direct comparison between field data and design/model predictions. The overall idea behind any SHM system is the evolution of the maintenance paradigm from periodic “time-based” NDE to “permanent-based” monitoring. Besides the scope of detecting damage at earliest possible stage, reliable SHM systems may monitor the loading conditions of a bridge to assess its performance under various service loads, to verify or update the rules used in its design stage, and to prioritize maintenance and rehabilitation. In any bridge SHM, sensors are mainly employed for monitoring external loading (wind, seismic, and traffic), structural responses (strain, displacement, and acceleration), and environmental effects (temperature, humidity, rain, and corrosion). The sensors are connected to dedicated hardware/software for storage and, in some cases, for real-time assessment.

Some researchers have defined the five main tenants to SHM (Napolitano *et al.* 2019): (1) defining the SHM plan, (2) installing the sensors, (3) maintaining the SHM system, (4) managing data and metadata associated with a system, and (5) closing out of the SHM system (if applicable). Others (Worden *et al.* 2007) have set - fundamental ‘axioms’, or general principles, to aid researchers, practitioners and owners in the design of SHM systems.

There has been a large volume of research on SHM and a comprehensive review of those works is well beyond the scope of this review article. A much fewer number of industrial routine applications exist, and these applications include different structures with very different requirements: rotating machine condition monitoring, global monitoring of large structures (structural identification), large area monitoring where the area covered is part of a larger structure, and local monitoring. The capabilities and potential applications of techniques in each category was discussed by Cawley (2018).

One of the challenges of SHM especially for long-span bridges is the challenge associated with the limitations of computational ability and the massive amount of data to be analyzed (Sun *et al.* 2020). To this end, big data and artificial intelligence techniques may offer viable ways to address the data interpretation problem. The interested readers are referred to a recent review paper by Sun

*et al.* (2020) who discussed the scope of big data analysis and artificial intelligence applied to bridge health monitoring.

The escalating progresses in SHM technologies has also led to the developments of standards and codes. For example, in 2016 the Chinese Ministry of Transportation published a new design code for SHM systems for new large highway bridges. This document is the first technical SHM code by a national government that mandates sensor installation on highway bridges. A summary of this code and other existing international technical SHM codes was given by Moreu *et al.* (2018). While there are several reports and documents recommending SHM systems, these same documents, according to Moreu *et al.* (2018), are not technically addressing SHM and sensor requirements. Table 1 in Moreu *et al.* (2018) lists bridge maintenance and monitoring codes and standards from Australia, China, Canada, European Union, Switzerland, UK, and the U.S. For the

Table 1 Bridges in the United States instrumented with sensing systems prior to 2011 according to Table 1.1 of Xu and Xia (2011)

#	Name	Location	Type	References	Sensor Type
1	<b>Golden Gate</b>	San Francisco, CA	Suspension	Pakzad <i>et al.</i> (Pakzad <i>et al.</i> 2008, Pakzad and Fenves 2009, Pakzad 2010); Chang and Pakzad (2013)	1,4,16
2	<b>Fred Hartman</b>	Houston Ship Channel, TX	Cable-stayed	Zuo and Jones (2005, 2010); Pure Technologies (2020); Texas Department of Transportation (2020)	1,2,3,4,5
3	<b>Sunshine Skyway</b>	Tampa Bay, FL	Cable-stayed	Agdas <i>et al.</i> (2015); Schenewerk <i>et al.</i> (2006); Mehrabi and Farhangdoust (2018)	2,3,5,7,9
4	<b>Quincy Bayview</b>	West Quincy (MO) – Quincy (IL)	Cable-stayed	Dong <i>et al.</i> (2010); Talebinejad <i>et al.</i> (2011);	9, 18
5	<b>Commodore Barry</b>	Chester (PA) – Logan Twn (NJ)	Truss	Kulcu <i>et al.</i> (2000); Pines and Aktan (2002); Catbas <i>et al.</i> (2008)	1,2,3,4,5,8, 12,19,21,22
6	<b>Ironton-Russell<sup>4</sup></b>	Ironton (OH) – Russell (KY)	Truss		2,3
7	<b>New Benicia Martinez</b>	San Francisco, CA	Box	Land <i>et al.</i> (2003)	2,3,4, 9,12,14
8	<b>Saint Anthony Falls I-35W</b>	Minnesota, MN	Box	French <i>et al.</i> (2012, 2014); Hedegaard <i>et al.</i> (2013, 2017a, b); Dalia <i>et al.</i> (2018); Gaebler <i>et al.</i> (2018); Inaudi <i>et al.</i> (2009)	2,3,4, 9,11,24
9	<b>North Halawa Valley</b>	Oahu, HI	Box	Robertson (2005)	2,3,5,12

<sup>4</sup> The original cantilever Ironton–Russell Bridge cited in Xu and Xia (2011) closed in 2016. It was replaced by a new white cable-stayed bridge has two lanes of traffic without a dedicated sidewalk (as the old one). The new bridge was opened on November 23, 2016. It is unclear whether or not the new bridge is under surveillance by an active SHM system.

latter, two documents are cited: Atkan *et al.* (2002) and Hooks and Weidner (2016). The latter is about the Long-Term Bridge Performance (LTBP) program, which is a long-term research effort to collect scientific performance data from a representative sample of bridges in the U.S. The data are collected from a variety of techniques and are supplemented with design plans, design and construction specifications, as-built plans and construction records, inspection and maintenance records, weather records, and traffic information. Although well detailed with all the protocols to be implemented, the LTBP does not account for specific SHM-oriented protocols but it rather focuses on NDE approaches, which are, by nature, time-based.

### 3. Bridge instrumentation program in the US

Xu and Xia (2011) listed sixty-three major bridges worldwide equipped with health monitoring systems, nine of which in the U.S. and shown in Table 1. The authors also identified the 25 different types of sensors listed in the note below Table 1. Table 2 complements Table 1 and lists bridges identified in the study presented here. It is noted here that the list of Table 2 was compiled to the authors' best knowledge.

In terms of sensing technology, Modares and Waksanski (2013) sorted SHM sensing systems by parameters, and provided details of sensor types, accuracy, range, and operating temperature. The considered parameters were (in alphabetical order): corrosion, cracking, displacement, fatigue, force, settlement, strain, temperature, tilt, vibration, water level, and wind. In addition, they classified the types of sensors as either contact or noncontact. With the progress in technology new sensing capabilities are developed and two excellent reviews on the subject were published by Sharyatpanahi (2015) and Moreno-Gomez *et al.* (2018), while a review focusing on sensors for concrete monitoring has been presented by Taheri (2019).

### 4. Bridge instrumentation review

The **Golden Gate Bridge** was instrumented with 64 wireless accelerometer-based sensor nodes distributed over the main span and the tower, collecting ambient vibrations synchronously at 1 kHz rate, in order to monitor vibration and identify mode-shapes. Each node consisted of four channels accelerometers in two directions and a microcontroller for processing and wireless communication. The initial testbed successfully proved the scalability of the network and the quality of the data, and was presented by Pakzad *et al.* (2008) who showed that the network was sufficiently dense and accurate to allow the identification of the modes of vibration. Over the years, the data from the wireless sensor network (WSN) were used to validate several statistical processing methods for modal identification (Pakzad *et al.* 2008, Pakzad and Fenves 2009, Pakzad 2010, Chang and Pakzad 2013).

~~~~~  
The twin-deck cable-stayed **Fred Hartman Bridge** has 192 grouted monostrand stays. After its completion in 1995, large-amplitude vibrations of the cables due to combined wind and rain effects were observed (Zuo and Jones 2005, 2010). Passive dampers and cross-ties were added to reduce the excessive vibrations. To evaluate these countermeasures, a SHM program was established in 1997 and included anemometers, rain gauges, accelerometers to monitor cable vibrations and deck vibrations separately, and load cells. The program revealed that the dampers

and cross-ties suppressed lower modes of vibrations induced by rain/wind, whereas they were less effective for the higher modes, which remained non-negligible (Zuo and Jones 2005). The program was complemented with a commercial acoustic sensors system, called SoundPrint<sup>®</sup> (Pure Technologies 2020), used to detect any wire breaks within the stays. Three sensors per stay were installed: one on each anchor and one on the stay approximately 2.5 m above the deck. The sensors were tethered to a dedicated data acquisition (DAQ) and management system located inside the North-East tower leg. According to the Texas Department of Transportation (2020), “*personnel have inspected some of the stays based on the reported wire events via anchorage investigations and stay force evaluations. To date, the inspections have not revealed significant changes in the measured stay forces due to the individual wire failures*”. It is not clear whether the monitoring program is still active or not.

~~~~~

Owing to its location, the **Sunshine Skyway Bridge** is vulnerable to high open channel winds. Multiple sensor types, including five GPS were installed to collect information about wind velocity and direction, concrete temperature, and overall bridge position (Agdas *et al.* 2015). The vibration of the stay cables were used to estimate cable tension while other data were used to calibrate a FEM to predict the bridge movement as a function of temperature and wind variances, and to set thresholds that would trigger alarms. Schenewerk *et al.* (2006) described the use of the GPS on the bridge. GPS receivers were placed at the top of the two bridge towers and at the midpoint of the center span; a fixed GPS reference site was established on the shore several miles away. Data were collected at 1 Hz rate. The findings from six months of monitoring indicated that the positions of autonomous sites located on a bridge can be measured automatically, with centimeter-level accuracies. Fifteen-minute measurements provide sufficient accuracy to reveal a complex variety of motions at each point monitored on the bridge. Laser-based measurements were used to detect the vibration of the cables and infer the force and the damping of the cables (Mehrabi and Farhangdoust 2018).

~~~~~

The **Quincy Bayview Bridge** is a cable-stayed bridge built in the late 1980s. Alike the Fred Hartman bridge, the cables were monitored with the SoundPrint<sup>®</sup> system (Dong *et al.* 2010). Talebinejad *et al.* (2011) proposed four damage detection algorithms to support the health monitoring program on this bridge. The algorithms were applied to numerical accelerations obtained from a linear elastic FEM implemented in ANSYS. Twelve damage scenarios at different locations of the deck and cables were modeled, and the corresponding mode shapes and natural frequencies were extracted. The four-damage identification strategies evaluated were the Enhanced Coordinate Modal Assurance Criterion (MAC), Damage Index Method, Mode Shape Curvature Method, and Modal Flexibility Index Method. Not all the identification strategies performed equally. Additionally, although none of the methods were able to predict multiple damages on the deck, the damage index method and the mode shape curvature method could precisely locate both single and multiple damage locations in the cables (Talebinejad *et al.* 2011). The study was not validated with any field data.

~~~~~

The **Commodore Barry Bridge**, opened in 1974, is the longest cantilever bridge in the U.S. (Catbas *et al.* 2008). It has a total length of 4,240 m and a main span of 501 m. Vibrating-wire (VW) accelerometers, strain sensors, weigh-in motion (WIM) devices, and tiltmeters were installed (Kulcu *et al.* 2000). Pines and Aktan (2002) used this bridge as a testbed for the framework of a supervisory control and DAQ system for SHM applications. Catbas *et al.* (2008)

developed a reliability model considering dead load, wind pressure, traffic loads, temperature effects and their combinations. The scope was to assess how health monitoring can be used to minimize the uncertainties related to phenomena which are difficult to model. For example, the study found that temperature-induced stresses on critical elements are not very easy to conceptualize and subsequently model. It was observed that the truss elements experience bending strains due to temperature. The peak-to-peak strain differential was observed to be around  $400 \mu\epsilon$ , which was about ten-fold higher than the maximum strains induced by traffic. Another outcome was that thermally-induced strains in this bridge cannot be neglected in any reliability estimation model.

~~~~~

The **New Benicia–Martinez Bridge** was opened in 2007 and measures about 2.7 km. Land *et al.* (2003) summarized the “when, what, and how” of the monitoring system designed to identify the time-dependent effects caused by creep and shrinkage. The long-span regions of the bridge were instrumented with 16-gauge stainless steel piano-wire serving as a reference line for span deflection. Linear variable displacement transducers (LVDTs) were attached to the piano-wire to measure the vertical deflection and axial shortening of span. Tiltmeters, VW strain gages, teflon-insulated thermocouples, center-hole load cells and acoustic sensing system were used to monitor rotation, concrete strain, temperature distributions, prestressing tendon and hinge bearing force and prestressing tendon fracture respectively. For measurement of steel cable corrosion, silver/silver chloride-based corrosion cells were used, and silver/silver chloride-based reference cell and polarization probe were adopted to monitor corrosion of footing and pier reinforcement. Besides Land *et al.* (2003), the peer-reviewed scientific literature about the SHM of this bridge is scarce.

~~~~~

The **I-35W St. Anthony Falls Bridge** is a concrete post-tensioned box girder structure opened in 2008 and constructed as two separate bridges built adjacent to each other, each consisting of four spans (French *et al.* 2014). More than 500 sensors of different types were installed to monitor deformations, temperature, vibrations, expansion, and corrosion. Deformations were measured with 198 VW strain gauges, 24 resistive strain gauges, and 12 fiber-optic strain gauges. Temperatures were measured by 246 thermistors some of which integrated into the vibrating-wire gauges. Twenty-six accelerometers measured vibrations while 12 linear potentiometers, located at the expansion joints, measured the overall expansion and contraction of the bridge. Electrochemical activity and concrete resistivity was also monitored to identify corrosion. For a detailed account of the location of the sensors, the interested readers are referred to Tables 2.1 and 2.2 of French *et al.* (2014).

Linear elastic FEM in ABAQUS were created and validated using truck-load tests (Hedegaard *et al.* 2013). It was demonstrated that local bending in the top flange had a large effect on how measured data compared with the computed results. It revealed that the strain profile at the centerline of the boxes was nonlinear for loadings located directly above and slightly offset from the instrumentation. Overall, the numerical results model compared well with respect to the truck test data. Hedegaard *et al.* (2013) recommended the use of additional instrumentation such as inclinometers near the bearings to quantify restraint caused by the bearings.

French *et al.* (2014) investigated the time-dependent (creep and shrinkage) and temperature-dependent behavior of the bridge to prevent excessive loss of post-tensioning that may yield to concrete cracking or large deflections. They used a combination of laboratory creep and shrinkage tests, in situ monitoring of longitudinal deflections and strains using the first five years of bridge operation, and FEMs. The results of this investigation were used to develop a prototype

monitoring system for the bearing movements using data from linear potentiometers located near the expansion joints on the bridge. Six time-dependent prediction models were used. Some of the conclusions were that the ACI-209 model overestimated the shrinkage strains by 50% whereas the 1990 CEB/FIP Model Code underestimated the shrinkage strains by approximately 22% over the entire duration of testing. Regarding creep, it was found that the laboratory creep strains were most accurately estimated by the 1978 CEB/FIP Model Code whereas the AASHTO LRFD provided accurate estimates up to 100 days after loading but underestimated the strains at later times.

It is noted here that the monitoring program for this bridge has been perhaps one of the most comprehensive reported in the literature. Interested readers are referred to (Dalia *et al.* 2018, Inaudi *et al.* 2009, French *et al.* 2012, 2014, Hedegaard *et al.* 2013, 2017a, b, Gaebler *et al.* 2018) for a holistic view of the lessons learned during this program.

~~~~~  
The **North Halawa Valley Viaduct** was instrumented during construction in 1994 with over 200 sensors distributed at seven different locations: VW strain gages, electrical resistance strain gages (ERSGs), thermocouples, extensometers, tendon load cells, base-line deflection systems, tiltmeters, and automated dataloggers. Embedded VWs were used to monitor concrete strain, Taut-wires measured vertical deflections of box-girders, and the extensometers measured the overall shortening of the box-girders (Robertson 2005). Vertical deflections and bending strains were measured during a load test and the results were compared with a FEM in SAP2000. Close agreement was observed for deflections and strains. Long-term deformations were compared with the analytical predictions of a FEM in SFRAME, specially developed for segmental construction of prestressed concrete bridge structures. This latter comparison showed that the theoretical predictions based on the original design parameters did not agree with the measured vertical deflections, and this was attributed to lack of adequate creep and shrinkage material properties.

~~~~~  
**1. The iconic Manhattan Bridge** has attracted increasing attention as a viable testbed for SHM systems, as multitudes of cracks have been observed over the years in the floor beams, at bottom chords of trusses, and stringers. Betti *et al.* (2014, 2016) conducted a monitoring program for one cable (cable D) and two panels of the bridge. The installation followed an inspection of the internal wires that determined that the wires were in good conditions with no breakage or degradation of the zinc coating. Overall, the monitoring system consisted of: (1) acoustic emission (AE) sensors; (2) two accelerometers to correlate any detected AE activity to bridge vibration and movement; (3) one weather station; (4) temperature/relative humidity sensors; (5) fiber optic strain gages; (6) deformation sensors; (7) wireless parametric sensor interface; (8) linear polarization resistance (LPR) sensors; (9) coupled multi-electrode corrosion sensor (CMAS) sensors and zinc sensors to collect corrosion rate. The fiber-optic gauges were placed along the suspension cable and two multiplexed strain and temperature deformation sensors mounted on the eyebars in the anchorage. For the panels, fiber-optic strain gauges were installed between panel point 1 and panel point 2 of cable D, relatively close to the anchorage. Each panel had also eight temperature/humidity sensors, four LPR sensors, four Corrosion Instrument bimetallic (BM) sensors, and two CMAS sensors. The sensors were assembled together on a plastic strap that was then placed inside the cable. During the 11 months monitoring campaign, the sensors performed well and demonstrated good durability. The corrosion sensors detected a potential onset of corrosion activity during a substantial snowfall followed by heavy rain. The BM sensors and the LPR recorded a spike in both zinc and steel corrosion rates. It took approximately 24 h before the corrosion rate returned to normal (i.e., no corrosion).

Babanajad *et al.* (2020) studied a portion of the Manhattan bridge to quantify the dynamic amplification generated by the rail joints and to observe the behavior of existing cracks. Fourteen strain gages captured flexural response, 16 strain gages measured shear response (8 rosette sensors). Six temperature sensors and four crack gages were also installed, the latter at locations prone to fatigue. A fiber-optic based SHM system was chosen for its high performance in terms of immunity to electrical/electromagnetic interference. The work of Babanajad *et al.* (2020) consisted of two phases. In the initial phase, a vibration survey served to identify locations of high and low dynamic amplification. In the second phase, the fiber optics were installed along with twenty accelerometers placed on select floor beams at several locations, near misaligned splices, as well as regions that had no alignment issues, for baseline comparison. The accelerometers were hardwired to a DAQ system, and operational acceleration was recorded for 30 train crossings. The data confirmed that the splices consistently cause an increase in acceleration. The monitoring was also used to quantify the impact of this amplification on the strain responses of the transit stringers and floor beams. The power spectra of the acceleration time-series showed: (1) a significant difference between data in the vicinity of smooth and misaligned joints; (2) how the amplitude of the acceleration varies with frequency. Overall, it was found that the lower the frequency the more the corresponding amplitude contributes to both displacement and stress. In the case of the transit stringer response, the misaligned joint resulted in up to 100% increase in amplitudes across all frequencies. In contrast, the responses of the floor beam show smaller increases in amplitude due to the misaligned joint, and these increases occur in the 25-50 Hz frequency range (Babanajad *et al.* 2020). The main outcomes of the monitoring period (May-June 2019) can be summarized as follows:

- The close spacing of wheel carriages on adjacent cars generates two superimposed cycles.
- Dynamic amplification levels in the transit stringer were well-correlated with the condition of the splices and linearly proportional with the speed of the train.
- While the large dynamic amplifications in the vicinity of the “severe” splices should not impact the fatigue life of transit or floor beams, they do result in very high localized stresses in the elements that connect the rails to the timber ties and the timber ties to the transit stringers. These stresses result in the failure of bolts and clips. Unless left unchecked, these local failures do not pose a threat to the structure itself, but do pose a falling hazard to those underneath the structure.
- An acoustic monitoring system is recommended to track the misalignment of splices in lieu of an acceleration- or strain-based monitoring system.

It is noted here that the **Manhattan Bridge** was also the subject of vision-based SHM. Interested readers are referred to (Feng and Feng 2017, Luo *et al.* 2018, Feng 2019).

~~~~~  
**2. Cracking problems were seen at various details of the Throgs Neck Bridge.** In response to these problems, Mahmoud *et al.* (2006) evaluated the fatigue life of the bridge, the retrofit schemes developed by Parsons Transportation Group (PTG), and calibrated a detailed 3D FEM also developed by PTG. Strain gages (to capture the local response of particular details and the global response of the instrumented spans), linear motion position sensors (to measure displacement), five uniaxial accelerometers, and thermocouple wires (to record surface temperatures on the underside of the deck plate and the top flange of the girder at the north and south ends of each monitored span) were installed. Measurements were taken under scheduled

trucks load and under random live loads for about a month. With a few exceptions, both the controlled tests and the live traffic indicated low stresses at the instrumented locations. Using the same instrumentation, the field stress and displacement measurements were used to compare the displacements of the retrofitted details with those of the non-retrofitted ones. Based on the field monitored data, time-dependent fatigue reliability assessment was made by Guo and Chen (2011) and Guo *et al.* (2012); S–N curves were used to consider the influence of variable amplitude loading on the propagation of initial defects and fatigue damage. It was observed that stress ranges measured at the instrumented details are all below the corresponding constant amplitude fatigue limits. Consequently, high fatigue reliabilities of these retrofitted details are expected.

~~~~~

3. In 1981, the **Vincent Thomas Bridge** was instrumented with an array of 26 accelerometers to measure ambient and earthquake vibrations. In 2006, a large cargo ship struck the bridge and induced moderate damage on a maintenance scaffolding at the main span. As the accelerometers were active prior to the event, the dynamic properties of the structure prior and after the collision could be assessed and showed that the impact did not create significant structural damage (Yun *et al.* 2008).

He *et al.* (2008) formulated a stochastic wind excitation model to study the modal response of the bridge using a 3D FEM. The natural frequencies, damping ratios, and mode shapes of the bridge were extracted and the effects of measurement noise on the system identification were included as well. The study did not include field measurements from the sensors installed on the bridge.

Torbol *et al.* (2013) selected this bridge as a test site for evaluating the wireless performance of a DuraMote sensing system developed and assembled in laboratory and consisting of data aggregators named Roocas and sensing nodes named Gopher. Three DuraMote sensors were placed symmetrically on the bridge: one in the middle and the other two approximately halfway between the towers and the center of the bridge. Each DuraMote consisted of one Roocas and two Gophers. Acceleration data, sampled at 1 kHz, were measured and recorded on the server for two hours from every sensing node. Frequency domain decomposition was used to analyze the data and extract the modal properties of the bridge.

~~~~~

4.5.6. The commercial SoundPrint<sup>®</sup> system was also used on the **Bear Mountain Bridge** and able to blindly identify and locate wire cuts and a number of wire breaks (Dong *et al.* 2010). Others bridges instrumented with a SoundPrint<sup>®</sup> system were the **Waldo Hancock Bridge** (demolished in 2013) and the **Bronx-Whitestone**. According to Dong *et al.* (2010) the system was able to monitor “*the deterioration of prestressing tendons*”, and “*cost-effective, targeted repairs have been carried out on a number of structures based on information generated by SoundPrint<sup>®</sup>*”.

~~~~~

7. The **Mackinac Bridge** was instrumented with a network of self-powered sensors and battery-powered wireless transmitters. The network prototype started collecting strain data in May 2017 and able to detect the increase in traffic due to the influx of bridge crossings during a local annual celebration. Owing to the short duration of the period monitored, there were no signs of drift (Aono *et al.* 2019). The wireless unit was improved by Faridazar (2019) and installed on the cross beams in the main suspended span, to measure dynamic events driving picowatt power dissipation. The technology, called piezo-floating-gate, is able to generate electrical energy created from mechanical vibrations. This energy is in part used to power all electronics in the sensing system, offering several advantages: (1) low power consumption, (2) self-powered continuous

sensing, (3) possibility of dense networks due to the small size of the sensors and the self-power capability, and (4) autonomous computation and nonvolatile storage of sensing variables (Faridazar 2019).

~~~~~  
**8.** The 1056 m long **New Carquinez Bridge**, a.k.a. the **Alfred Zampa Memorial Bridge** is a suspension bridge with a main span of 730 m. Just prior to its opening, in November 2003, a set of dynamic field tests was performed for system identification (Conte *et al.* 2008, He *et al.* 2009). The tests included ambient vibration, mainly wind induced, and forced vibration under four different controlled traffic load patterns and seven different vehicle-induced impact load configurations. The dynamic response of the bridge was measured through an array of 34 uniaxial and 10 triaxial force-balanced accelerometers installed along the whole length of the bridge. The modal characteristics (natural frequencies, damping ratios, and mode shapes) were extracted using the natural excitation technique-eigensystem realization algorithm, the stochastic subspace approach, and the enhanced frequency domain decomposition algorithm.

A permanent wired seismic monitoring system was installed in 2004. It includes 27 sensors on the approach, 1 anemometer, and 76 force balance accelerometers on the suspension bridge. The latter were distributed along the main span, towers, and foundations (Hong *et al.* 2011, Nagarajaiah and Erazo 2016). A separate wireless structural monitoring system was installed in 2010 (Kurata *et al.* 2013) to collect data on a regular basis (e.g., schedule-based). It uses the Narada wireless platform developed at the University of Michigan (Swartz *et al.* 2010), and is able to support four sensing channels with a 16-bit resolution. The long-term wireless structural monitoring system was designed to record bridge responses (i.e., strains, displacements, and accelerations) and environmental conditions (i.e., temperature, wind speed, and wind direction). Thirty-five Narada sensor nodes collecting data from 76 sensing channels were installed. To measure the vertical and transverse motion of the orthotropic steel deck, 19 triaxial accelerometers were installed along the deck. At the top of each tower, two triaxial accelerometers measuring one vertical, one transverse, and two longitudinal degrees-of-freedom were also installed. To measure strain of the orthotropic steel deck, metal foil strain gauges were mounted to the interior surface of the box girder at three locations along the span: over the north and south towers and approximately at midspan. At each location, three strain gauges were installed to measure longitudinal strain on the top and bottom girder surfaces and transverse strain on the top surface. For thermal compensation, three thermistors measured the top and bottom girder surface temperatures and ambient internal air temperature of the girder. To capture the longitudinal displacement of the steel orthotropic deck relative to the concrete towers, three string potentiometers were installed: two at the south tower and one at the north tower. Three weather stations were also installed each consisting of one anemometer, additional environmental sensors (either a wind vane, thermistor, or humidity sensor). In total, 46 channels of acceleration, 10 channels of strain, 3 channels of displacement, and 17 channels of environmental parameters (i.e., wind speed, wind direction, temperature, and humidity) were installed.

Zhang *et al.* (2017) used the data collected from the wireless system in a stochastic identification approach for the extraction of the modal characteristics. Ridge regression and Gaussian process regression were used to model the dependency of modal frequencies on bridge environmental and operational conditions using bridge responses, wind speed and direction, and bridge temperature collected between 01/01/2013 and 12/21/2014. Twenty-seven operational modes were identified, 15 of which corresponded to modes previously reported. With the accurate estimation of the modal frequencies, the median modal frequency and damping ratio of each mode

were determined. The empirically derived distributions for modal damping revealed that the mode of the distributions for most structural modes were well below 0.8% with many low-order modes less than 0.3%. The results proved that the 0.3% damping ratio used in the design of the bridge was a reasonable value. The modes also exhibited sensitivity to environmental conditions.

~~~~~

**9.** The 1206 m long **Bill Emerson Memorial Bridge** opened in 2003. Its monitoring began one year later with a seismic instrumentation made of 84 accelerometers (Hartnagel *et al.* 2006). The data from a May 1, 2005, M4.1 on a Richter scale earthquake, were used to validate a 3-D FEM in SAP2000 (Chen *et al.* 2007). Peak ground and structure accelerations were retrieved from the instrumentation to assess the condition of the structure under an earthquake, and to develop and validate the model. The main conclusions of the study were:

- The algorithm used was able to extract frequencies and mode shapes.
- Cables and bearings significantly influence the stiffness of the bridge.
- Cables sagging should be considered in the modeling to account for geometric nonlinearities.
- Most of the vibration modes are coupled with others, and the measured frequency and mode shapes indicate that the cable-stayed structure is most flexible in the vertical direction and least flexible in longitudinal direction.
- The 31 significant modes of vibration up to 14.09 Hz include more than 70% mass participation in translational and rotational motions along any of three directions. The fundamental frequency is 0.339 Hz, corresponding to vertical vibration of the main bridge. Cables begin to vibrate severely at a natural frequency of 0.842 Hz or higher.
- The mass density of concrete and boundary conditions are the key parameters affecting the modal properties of the bridge.
- The computed natural frequencies of the 3-D FE model agree well with the field measurements with maximum error within 10%.

~~~~~

**10.** The old **U.S. Grant Bridge** was closed in 2001 for demolishing. Its replacement (**Fig. 1**) was completed in 2006. During construction, the new bridge was instrumented with different types of sensors, whose locations were chosen using original design calculations and erection analysis (Helmicki and Hunt 2013). The following variables were monitored: weather; thermal cross-section of pylons, exterior girders, and concrete-decking sections; longitudinal and tangential stress at pylon cable anchorages; tip displacement of the outermost-decking sections in response to thermal, wind, and dead load in order to ensure proper alignment; dynamics of the stays. Helmicki and Hunt (2013) reported that most of the monitored segments exhibited a relative agreement with the design values.

Once opened to traffic, the monitoring system remained active when the Kentucky abutment and backwall began to exhibit cracking that started near the beam seat but became pervasive with increasing length and width over each subsequent inspection. This degradation was attributed to field modification to the location and installation of the steel pulldowns internal to the abutment. The rehabilitation, completed in 2009, included additional welding at the beam seat to resist further movement. A truckload test was conducted to evaluate the rehabilitation and compare with expected design values. Some of the strain gages detected a significant change in the truck response near the abutment: the post-rehabilitation influence line exhibited a more pronounced middle span response and an increased tensile bias in the Kentucky end-span, as compared to the baseline. This “new” influence line was used to re-calibrate a FEM developed previously.



Fig. 1 The U.S. Grant Bridge. Credity <http://feinknopf.photoshelter.com/image/I0000cvarWU9ouEg>

Compared to baseline data, the measured results showed a decrease at the middle span and an increase at the Kentucky abutment.

In January 2011, tiltmeters were installed upon the abutment wall to document long-term effects such as daily temperature swings. In June 2011, strand meters were mounted immediately after the installation of exterior pulldowns to measure the axial displacement within a steel strand. A strain gage was also installed on each pulldown for redundancy and to improve accuracy. Accelerometers were also placed on the cable's protective cover pipe to estimate the cable force using the vibrating chord theory. This was done under the assumption that the cables move in unison with the internal wire strands. Except for a few cables, the difference between the empirical estimation and the design tensions were found to be below or well below 10% (see Fig. 9.10 of Helmicki and Hunt 2013). Some data analysis about the U.S. Grant Bridge can also be found at (Norouzi *et al.* 2014).

~~~~~  
**11. The Charles W. Cullen Bridge** is a 533 m long cable-stayed bridge with a 289 m main span and two 121 m back spans. The bridge was opened in 2012 with a comprehensive SHM system based on fiber optics with: 70 strain sensors, located in the edge girders, pylons, and deck; 44 accelerometers mounted to the deck, pylons, and stay cables; 9 tiltmeters mounted along the east edge girder; 3 displacement sensors, one at each of the bridge expansion bearings (Shenton *et al.* 2013, 2016, 2017, Al-Khateeb *et al.* 2019). The system was completed with two types of non-fiber-optics based sensors: 2 anemometers, one at deck level and one at the top of one pylon; 16 chloride sensors in the deck. To guarantee survivability, some strain sensors were embedded in the concrete.

Al-Khateeb *et al.* (2019) presented the results of six load tests performed just prior to the bridge's opening, and then again at 6 months, 1, 2, 4, and 6 years. The results of the first two tests established the baseline performance, as the second test showed that the bridge response stabilized. In order to eliminate any initial offset, the time-history record was first "zeroed" by taking the average of the first 25 data points and subtracting that value from the entire time history. Then, a moving average was computed using a window of 25 data points to eliminate the inherent low-level noise in the sensor data. Finally, the maximum and minimum (i.e., peak) values of the record were determined. From the strains, the stress was obtained by multiplying strain to the Young's modulus of 200 GPa for steel and 35.6 GPa for concrete. The latter was obtained by averaging the compressive strength found by testing concrete cylinders at the time of the construction. The baseline peak strains for single, four, and six truck passes was determined (see Table 2 of Al-Khateeb *et al.* 2019). At the end of the six-year experimental campaign, Al-Khateeb *et al.* (2019)

Table 2 Bridges in the United States instrumented with sensing systems prior/after 2011 but not included in Xu and Xia (2011)

#	Bridge Name	Location	Type	References	Instrumentation
1	<b>Manhattan Bridge</b>	New York, NY	Suspension	Babanjad <i>et al.</i> (2020); Betti <i>et al.</i> (2014, 2016); Feng and Feng (2017); Luo <i>et al.</i> (2018); Feng (2019)	acoustic emission sensors; accelerometers; weather station; temperature/relative humidity sensors; fiber optic strain gages; deformation sensors; linear polarization resistance sensors; corrosion sensor; crack gages
2	<b>Throgs Neck Bridge</b>	New York, NY	Suspension	Mahmoud <i>et al.</i> (2006); Guo and Chen (2011); Guo <i>et al.</i> (2012);	strain gages; linear motion sensors; uniaxial accelerometers; thermocouple wires.
3	<b>Vincent Thomas Bridge</b>	Los Angeles, CA	Suspension	Yun <i>et al.</i> (2008); Torbol <i>et al.</i> (2013); He <i>et al.</i> (2008)	accelerometers
4	<b>Bear Mountain Bridge, a.k.a. Purple Heart Veterans Memorial Bridge</b>	Fort Montgomery, NY	Suspension	Dong <i>et al.</i> (2010)	acoustic sensors: SoundPrint® system
5	<b>Waldo-Hancock Bridge (now demolished)</b>	Verona, ME	Suspension	Dong <i>et al.</i> (2010)	acoustic sensors: SoundPrint® system
6	<b>Bronx-Whitestone</b>	New York, NY	Suspension	Dong <i>et al.</i> (2010)	acoustic sensors: SoundPrint® system
7	<b>Mackinac Bridge</b>	Connect the Upper and Lower Peninsulas of Michigan	Suspension	Aono <i>et al.</i> (2019); Faridazar (2019)	
8	<b>Alfred Zampa Memorial (New Carquinez)</b>	Vallejo, CA	Suspension	Nagarajiah and Erazo (2016); Zhang <i>et al.</i> (2017); Hong <i>et al.</i> (2011); Kurata <i>et al.</i> (2013); Conte <i>et al.</i> (2008), He <i>et al.</i> (2009)	tri-axial accelerometers; anemometer; strain gages; thermistors; humidity sensors;

9	<b>Bill Emerson Memorial Bridge</b>	Connecting MO Route 74 with IL Route 146 across the Mississippi River	Cable-stayed	Hartnagel <i>et al.</i> (2006); Chen <i>et al.</i> (2007)	accelerometers; weather station
10	<b>U.S. Grant Bridge</b>	Portsmouth (OH) over the Ohio river	Cable-stayed	Helnicki and Hunt (2013); Norouzi <i>et al.</i> (2014)	accelerometers; strand meters; strain gages; tiltmeters
11	<b>Charles W. Cullen Bridge aka Indian River Inlet Bridge</b>	Indian River Inlet, Sussex County, Delaware	Cable-stayed	Shenton <i>et al.</i> (2013, 2017); Al-Khateeb <i>et al.</i> (2019); Wu <i>et al.</i> (2019); Natalicchio (2018)	fiber optics sensors that included: strain sensors, accelerometers, tiltmeters, displacement sensors
12	<b>Varina-Enon Bridge</b>	Hopewell, VA	Cable-stayed	Maguire (2013); Maguire <i>et al.</i> (2018)	strain gages; LVDT; crack sensors; temperature sensors
13	<b>Northbound US 41 over Ohio River</b>	Henderson Co., KY	Truss	Peiris <i>et al.</i> (2018)	LVDTs; triaxial accelerometers;
14	<b>Albert Gallatin Memorial</b>	Point Marion, PA	Truss	GEOKON (2020); CANARY (2020)	inclinometers; vibrating wire piezometers;
15	<b>Government Bridge or Arsenal Bridge</b>	Rock Island, IL to Davenport, IA	Truss	Dong <i>et al.</i> (2010)	accelerometers; acoustic emission sensors; corrosion sensors; optical sensors (strain and temperature measurements), weather station
16	<b>World War I Memorial Bridge</b>	Portsmouth (NH) to Kittery (ME) over the Piscataqua River	Truss	Shahsavari <i>et al.</i> (2019, 2020); Chen <i>et al.</i> (2018)	accelerometers; uniaxial strain gauges; eleven strain rosettes; tiltmeters
17	<b>New Hope-Lambertville Toll-Supported Bridge</b>	New Hope (PA) to Lambertville (NJ)	Truss	GEOKON (2020)	wire strain gauges; tiltmeters
18	<b>Riverton–Belvidere Toll- Supported Bridge</b>	Riverton (PA) to Belvidere (NJ)	Truss	GEOKON (2020); Chang <i>et al.</i> (2011)	wire strain gauges; tiltmeters
19	<b>Burlington-Bristol Bridge</b>	Bristol (PA) to Burlington (NJ)	Truss	De Roeck <i>et al.</i> (2011); Campbell Scientific (2020a)	accelerometers; electrical resistance strain gages; vibrating-wire strain gauges; vehicle-speed sensors; road-surface temperature sensors

20	<b>Chulitna River Bridge</b>	Trapper Creek, AL	Steel plate girder	Xiao <i>et al.</i> (2017)	fiber optics sensors; strain gages; accelerometers; displacement sensors and tiltmeters
21	<b>Bridge 1-813, I-495 over the Christina River</b>	Wilmington, DE	Steel plate girder	GEOKON (2020); McNeil <i>et al.</i> (2019)	tiltmeters
22	<b>I-64 over US 60</b>	Franklin Co., KY	Steel plate girder	Harik and Peiris (2013); Peiris <i>et al.</i> (2018)	accelerometers; strain gauges
23	<b>I-24 over Tennessee River</b>	Marshall Co., KY	Steel arch and plate girder	Peiris <i>et al.</i> (2018)	LVDI; temperature sensors; tiltmeters.
24	<b>I-39 Wisconsin River</b>	Wausau, WI	Steel plate girder	Mahmoud <i>et al.</i> (2005); Liu <i>et al.</i> (2009); Orcesi and Frangopol (2011)	ERSGs; LVDTs
25	<b>P-0962 bridge</b>	Dallas County, MO	Steel girder	Watkins <i>et al.</i> (2007)	EFPI strain sensors; ERSGs
26	<b>C-846 Bridge</b>	Salt Lake City, UT	Steel girder	Halling and Petty (2001); Nichols (2017); Nichols <i>et al.</i> (2018)	bi-axial and tri-axial accelerometers; thermocouples
27	<b>Interstate 91 (I-91) northbound. Meriden Bridge</b>	Meriden, CT	Steel girder	Christenson and Motaref (2016); Jin <i>et al.</i> (2015, 2016); Xiao <i>et al.</i> (2020); Lobo-Aguilar <i>et al.</i> (2019)	foil strain gages; piezoelectric strain sensors; piezoelectric accelerometers; capacitance accelerometers with additional temperature sensing capability; resistance temperature detectors
28	<b>US 30 Highway (Iowa)</b>		Steel girder	Seo <i>et al.</i> (2013); Lu <i>et al.</i> (2010); Wipf <i>et al.</i> (2007a, b)	fiber optics strain sensors
29	<b>Crum Creek Viaduct (Rail bridge)</b>	Swarthmore, PA	Steel girder	IIS (2020); GEOKON (2020)	vibrating wire gages
30	<b>Telegraph Road</b>	Monroe, MI	Slab-on-girder highway bridge	Hou <i>et al.</i> (2020a, b); O'Connor <i>et al.</i> (2017)	accelerometers; strain gauges; and thermometers
31	<b>Carroll Lee Cropper</b>	Boone County, KY	Continuous steel arch-shaped truss	Peiris <i>et al.</i> (2018)	vibrating wire microcrack meters

32	<b>Huey P Long bridge</b>	Bridge City, LA	Cantilevered steel through-truss	Weinmann (2015); Kleinahns (2009)	strain gages
33	<b>Tacony-Palmyra Bridge</b>	Tacony (PA); Palmyra (NJ)	Steel tied arch and double-leaf bascule	Yarnold <i>et al.</i> (2012b); Yamold and Moon (2015)	vibrating wire strain gages; crack meters
34	<b>Streicker Bridge (Pedestrian bridge)</b>	Princeton, NJ	Steel arch and reinforced, post-tensioned concrete	Glisic (2018); Napolitano <i>et al.</i> (2019); SMARTEC (2017b)	discrete FBG long-gauge sensors; distributed Brillouin Time Domain Analysis sensors; FBG-based strain sensors; sensing sheets
35	<b>Fremont Bridge</b>	Portland, OR	Steel-tied arch	Campbell Scientific (2020b)	strain and surface temperatures sensors
36	<b>Neville Island</b>	Pittsburgh, PA	Steel-tied arch	Connor <i>et al.</i> (2005); Kwon and Frangopol (2010)	accelerometers; LVDTs; uniaxial ERSG
37	<b>Birmingham Bridge</b>	Pittsburgh, PA	Bowstring arch	Kwon and Frangopol (2010); Connor and Fisher (2001); Liang and Chen (2014); Connor <i>et al.</i> (2004, 2005)	accelerometers; LVDTs; Uniaxial ERSG
38	<b>Cedar Avenue Bridge</b>	Burnsville, MN	Tied arch	Schultz <i>et al.</i> (2014)	acoustic emission sensors
39	<b>New Mexico I-10 Bridge</b>	Las Cruces, NM	Steel deck arch	SMARTEC (2020)	fiber optics strain gages
40	<b>Columbia River I-5 Bridge</b>	Portland, OR	Steel vertical-lift, "Parker type" through-truss	Campbell Scientific (2020c)	tiltmeters; laser position sensors
41	<b>NBI# 000000003231620</b>	Potsdam, N.Y. (Carrying Wright Road over Trout Brook)	Reinforced concrete slab	Whelan <i>et al.</i> (2009)	MEMS accelerometers; strain transducers
42	<b>New Nibley Bridge</b>	UT	Precast deck T-girders	Alder <i>et al.</i> (2018); Pace <i>et al.</i> (2019)	strain gages; thermocouples; accelerometers; geophones velocity transducers
43	<b>New Trammel Creek</b>	Allen County, KY	Integral abutment	Peiris <i>et al.</i> (2018); Zhu <i>et al.</i> (2015)	pressure transducers; temperature gauges; tiltmeters

44	<b>Lambert Road Bridge</b>	Sacramento, CA	Integral abutment	Barr <i>et al.</i> (2012); Foust (2014); Foust <i>et al.</i> (2014)	Hitec strain gauges; geokon vibrating-wire strain gauges; velocity transducers (geophones); tiltmeters; thermocouples
45	<b>I-65 elevated expressway</b>	Jefferson Co., KY	PC I-girder bridge	Peiris <i>et al.</i> (2018)	LVDTs
46	<b>Powder Mill Pond, a.k.a. Vernon Avenue Bridge</b>	Barre, MA	3 Span Steel Girder	Kaspar (2018); Ahlborn <i>et al.</i> (2010); Santini Bell <i>et al.</i> (2010); Sanayei <i>et al.</i> (2012)	strain gauges; girder thermistors; concrete thermistors; bi-axial tiltmeters; accelerometers
47	<b>Rio Puerco bridge</b>	Albuquerque, NM	Precast, prestressed I-beam girders	SMARTeC (2017b)	fiber optics (SOFO) to measure prestress
48	<b>San Ysidro Bridge</b>		Precast, prestressed I-beam girders	Barr <i>et al.</i> (2006)	strain gages
49	<b>Horsetail Falls bridge</b>	Multnomah County, OR	Pre-stressed concrete	Soltész (2002), Kachlakev and McCurry (2000), Kachlakev <i>et al.</i> (2001)	bragg grating strain gages
50	<b>Sylvan Bridge</b>	Oregon (ODOT Bridge No. 02285)	Pre-stressed concrete	Soltész (2002), Kachlakev and McCurry (2000), Kachlakev <i>et al.</i> (2001)	fiber optics strain gages
51	<b>Kishwaukee River Bridge</b>	Winnebago County, Illinois	Pre-stressed concrete box girder	IIS Inc. (2020)	strain gages; accelerometers; clip gages; LVDT gages
52	<b>Watson Wash bridge</b>	Mojave Desert, CA	RC T-girder bridge	Lee (2005); Lee <i>et al.</i> (2007)	accelerometers
53	<b>Kings Stormwater Channel bridge</b>	Riverside County, CA	Concrete-filled carbon/epoxy tubes girder	Guan <i>et al.</i> (2006)	accelerometers; strain gages; linear potentiometers; temperature sensor; pan tilt-zoom camera
54	<b>Penncoy Viaduct</b>	Philadelphia, PA	Steel multi-girder	Furkan <i>et al.</i> (2020)	displacement string potentiometers sensors
55	<b>Sunrise Boulevard Bascule Bridge</b>	Fort Lauderdale, FL	Bascule Bridge	Catbas <i>et al.</i> (2010, 2012); Catbas and Malekzadeh (2016)	dynamic strain gages

reported that the comparisons of time histories, peak values, and distribution factors indicate that the bridge condition has remained unchanged. Although the data contained some variability, no trends were observed.

Natalicchio (2018) built and calibrated a 3D FEM in STAAD.Pro using empirical strain data from the controlled load tests. The calibrated parameter was the elastic modulus of the edge girders. Through various iterations, the optimized model of the bridge showed good results when compared to the SHM strain response and the concrete edge girder 56-day compressive strength tests. The model was validated using different loading configurations, and it proved to be a closer representation of the structure. Wu *et al.* (2019) proposed the development and application of sensor placement optimization methods, which have been integrated and implemented in a versatile software tool for maximizing the sensor coverage capacity for structural performance assessment. The proposed optimization was “virtually” applied to this bridge.

~~~~~

**12.** In 2012, inspectors noticed a significant flexural crack opening, visually estimated at 1.5 mm under traffic, on the last span of the approach of the 1426 m long **Varina-Enon Bridge**. Other significant flexural cracking were observed at several locations on the northbound approach. Many of these cracks were through or near the epoxied joints propagating vertically from the bottom flange and through the web. Other noticed issues were segment-to-segment joint opening on the end span of the first approach structure (Maguire 2013, Maguire *et al.* 2018). To investigate causes, live-load testing and long-term monitoring (09/2012 through 01/2014) were completed. Seventy-seven total strain, crack displacement, deflection, and temperature sensors were used. A simple matrix structural analysis was used to compare measured and calculated strains and displacements. In the beamline model, the southernmost support was pinned and the remainder were assigned rollers. While for the rebar and the prestressing steel, the modulus of elasticity was assumed equal to 200 GPa and 197 GPa, respectively, the modulus of concrete was set at 34 GPa after due calibration with field data.

The long-term monitoring consisted of collecting data based on loaded induced events, which were triggered when the strain response exceeded a threshold of  $12 \mu\epsilon$  (413 kPa, assuming  $E_{concrete} = 34 \text{ GPa}$ ) at the middle of the bottom slab at certain specified section. This threshold was set to be similar to a single truck crossing based on the results from the load test. Once an event was triggered, the logger recorded 1.8 seconds before and after the threshold was exceeded, that was deemed effective at recording the entire event for vehicles traveling at highway speed. For each event the data from the strain transducer, LVDTs at the crack opening, concrete temperature, and maximum differential temperature were recorded. The data logger zeroed the strain transducers every 30 s unless a significant crossing was identified, and then checks again after an additional 30 s. Over 17 months monitoring program, 6,021 events were recorded. Maguire *et al.* (2018) concluded that:

- The live-load test did not reproduce the expected magnitude of longitudinal crack displacement.
- There were 389 crack openings 0.0625+ mm, with the largest equal to  $\sim 0.76$  mm.
- The analysis indicates that the locations where cracking and joint opening occurred have higher tensile stresses under the combination of live load plus positive thermal gradient.

~~~~~

**13.** The **northbound US 41 bridge (NB US 41)** is a cantilever through-truss bridge, 1950 m long, instrumented to monitor the piers for impacts from barges (Peiris *et al.* 2018). Triaxial

accelerometers were mounted on the top of three piers along the northbound side; LVDTs were mounted on the expansion bearings atop one of the three piers. Video equipment recorded visual evidence of any impact. Typical data collected during the 2006–2015 monitoring period included acceleration, displacement, and videos. A plot of the time history for the accelerations and displacements immediately prior to (~ 2-5 sec) and following impacts (~ 15-30 sec), as well as maximum hourly acceleration and displacement data, were made accessible through a website. Various acceleration and displacement thresholds were set to identify severe and/or critical impacts. Acceleration larger than 0.2 g was labeled as a severe impact, i.e., an impact that would cause possible damage to the piers in question. The data storage was activated once a 0.05 g impact was detected. According to Peiris *et al.* (2018) the system was questioned when neither the impact of a barge on April 2008 nor an earthquake occurred a few days later activated the data storage.

~~~~~  
**14.** The Albert Gallatin Memorial Bridge was an old truss structure that was imploded in 2009 and replaced with the new **Point Marion Bridge**, opened in 2009. The soft soil surrounding the foundation prompted a monitoring program to observe the impact of new bridge construction on the aging structure (GEOKON 2020). Nineteen VW piezometers monitored water pressures in the foundation soils on both sides of the river, while a VW piezometer recorded river water levels, and two VW strain gages monitored the old bridge. Manual measurements were taken of tilt plates, settlement pins (placed in the fill) and inclinometers installed in the foundation soils (GEOKON 2020). Data were automatically collected and imported into a MultiLogger on an hourly basis while a dedicated software was used to provide the construction contractor and owner with access to data via the Internet. Some details about the monitoring program are available at (CANARY 2020).

~~~~~  
**15.** The **Arsenal Bridge** or **Government Bridge** was completed in 1896 and includes a swing section to accommodate traffic navigating the locks. This Pratt truss structure was instrumented to monitor the effects of traffic and heavy truck loads using an optical Interrogator, 36 optical strain sensors, 21 optical temperature sensors, 10 optical accelerometers, and one fiber optic tiltmeter. Conventional AE sensors, weather station, and corrosion sensors were also installed. A map of the installation is visible in Dong and co-authors (2010).

~~~~~  
**16.** The **World War I Memorial Bridge** (Fig. 2) is a vertical-lift bridge opened in July 2013. Shahsavari *et al.* (2019) described a SHM program that began in March 2017 to observe the: (1) dynamic performance of the horizontal span and the lift tower; (2) strain distribution through the gusset-less connection for design verification and fatigue performance assessment; (3) effects of corrosion on load-carrying capacity. Twelve accelerometers, uniaxial strain gauges, eleven strain rosettes, and tiltmeters were installed. The accelerometers monitor the vibrations along the length of the horizontal span and height of the tower. The rosettes at two gusset-less connections on the span and at the three joints on the tower determine the force path through the webs of the connections. The uniaxial gauges, mounted on a diagonal member connecting the instrumented connections on both east and west faces of the bridge, assess the symmetric behavior of the bridge. The tiltmeters monitor the tower movement due to wind, bridge lifts, and combinations of the two.

Shahsavari *et al.* (2020) presented a decision-making protocol for assessing structural behavior and capacity under various damage scenarios. A 3D FEM in SAP2000 was built and calibrated using the SHM data collected from a controlled truckload test. The model was used as a benchmark to: (1) assess the global response of the bridge as a function of damage level; (2)



Fig. 2 The World War I Memorial Bridge. (Credit: Ken Gallager at English Wikipedia, CC BY-SA 3.0 <https://commons.wikimedia.org/w/index.php?curid=48356074>)

investigate the load-carrying capacity of the bridge subject to damage; and (3) determine whether the damaged members comply with the bridge analysis and design code provisions for combined axial and flexural effects.

The numerical accelerations were decomposed at multiple frequency resolutions using the wavelet packet transform. Shahsavari *et al.* (2020) hypothesized that the energy rate indexes of all wavelet packet components vary significantly due to an abnormal change in the global performance or in-service condition of the bridge. The 3D model was calibrated by running a controlled pseudo-static load test using a dump truck with a gross weight of 17,690 kg. With the bridge temporarily closed to traffic, data were sampled at 100 Hz. To reduce uncertainty and variability on data reading due to sensor bias (small offset in the signal average output), before performing the load test, all sensors were calibrated to ensure collecting reliable data. The pseudo-static test was designed with two stopping positions on each lane of the bridge. Several simplifications were made in the model but still the modal and static numerical predictions matched fairly well with the field observations (see Tables 1 and 2 of Shahsavari *et al.* 2020). Different damage scenarios were simulated: truck accident (A), vessel collision (B), fatigue damage (C), and loose bolts (D).

It is noted here, that Chen *et al.* (2018) measured the displacements due to the lift using video cameras located 80+ m away, to extract vibration frequencies and mode shapes of the bridge. The measured signals were compared with those from accelerometers and strain gauges installed on the bridge, and identified characteristics of the bridge were compared to a FEM.

~~~~~  
**17. and 18.** Owing to their age (100+ years old) and similar structural properties, the **New Hope-Lambertville Toll-Supported Bridge** and the **Riverton–Belvidere Toll-Supported Bridge** were selected to test a monitoring system (GEOKON 2020) able to detect and enforce oversized vehicles. VW strain gauges and tiltmeters were installed and connected to a data logger utilizing a 8-channel dynamic VW analyzer. The data were compared against a FEM. A controlled load test was conducted on each structure to set the baseline and calibrate the model, after which a short-term monitoring study was carried out to assess performance under vehicle and environmental loadings, and to assess the ability to identify overweight vehicles. During a month of monitoring, several significant vehicle crossings were identified and properly labeled to oversized vehicles.

The system was then used to determine if these crossings changed the behavior of the structure, which could be indicated by some nonlinearity induced by the vehicle (GEOKON 2020). Chang *et al.* (2011) used the acceleration data from a WSN installed on the **Riverton-Belvidere bridge** to validate a framework for system identification. Eight nodes were installed on the main span, four on each side, to identify vertical, torsional, and transverse modes. The accuracy of the algorithm was estimated through the distribution of the identified vibration frequencies, damping ratios, and mode shapes which equally contribute to quantify the accuracy of the proposed algorithm. Four stochastic modal identification methods were used to identify modal parameters of the bridge and examine the identified results.

~~~~~  
**19.** The **Burlington-Bristol Bridge**, built in 1931, consists of a main 165 m steel through-truss vertical lift span with adjacent 61 m steel through truss tower spans (De Roeck *et al.* 2011). Two laser displacement sensors measured the movement of the movable lift span, a water-level sensor produced real-time under-clearance measurements of the bridge, and ERSGs, VW strain gages, vehicle-speed sensors, and road-surface temperature sensors completed the SHM instrumentation (Campbell Scientific 2020a), which was supplemented by a detailed 3D FEM of the entire span.

De Roeck *et al.* (2011) conducted a numerical and an experimental structural identification study. The three main spans were modeled individually in SAP2000 and used in conjunction with the preliminary data collected in the field to identify key uncertainties as well as the nodal points, amplitude and bandwidth of the mode. The models were created using frame and shell elements and the results were compared against field vibration measurements collected during the summer of 2009 at the five different locations. Forty-five accelerometers (30 piezoelectric and 15 capacitive) were hardwired into a DAQ system, with sampling rate set at 200 Hz, sufficient to recognize the highest anticipated natural frequency of interest below 20 Hz. The field data were processed using stochastic subspace identification to estimate natural frequencies and mode shapes that, in turn, were used to globally calibrate the FEM. Owing to uncertainties related to the modeling of each span constructed and analyzed separately, a comprehensive model of the entire bridge including approaches was constructed in Strand7. This model was then calibrated to globally match the experimental data. In analyzing the measured time histories of each of the spans under ambient vibrations, it was noted that the two tower spans had similar mode shapes and frequencies, but the magnitude of their acceleration time histories were different. The peak lateral vibration of the top chord on the NJ Tower Span was roughly four times the magnitude of corresponding lateral vibration on the top chord of the PA Tower Span, while each of the bottom chord lateral and vertical accelerations were of equal magnitude. This difference was attributed to the foundation types of the piers. Another finding of the study was that the analytical acceleration response obtained from Strand7 model matched well the response to a truck load dynamic test. The study also demonstrated that the perceived vibration difference between the two spans was a real phenomenon and attributed to the fact that the spans are not exactly symmetrical, due to differences in the way the super-structures are supported by the sub-structures and in the lateral stiffness provided by the adjacent spans (De Roeck *et al.* 2011).

~~~~~  
**20.** To monitor the effects of extreme temperatures, the 240 m long **Chulitna River Bridge** was equipped with fiber optics sensors, strain gages, accelerometers, displacement sensors and tiltmeters (Xiao *et al.* 2017). Located in Alaska, this bridge endures large temperature swings (from a highest 96°F to a lowest of -34°F), flooding, and snow amounts measured in meters. Eight optical rosette strain sensors were used in conjunction with twelve optical strain sensors to

evaluate the bending and shear forces along the piers and at the midspan of the girders. Fifteen optical strain sensors, placed along the composite structures, evaluated bending and axial forces. Twelve additional optical strain sensors were located on the diagonal trusses of the cross frame as well as along the concrete deck. Five accelerometers were used to determine the change in stiffness within the trusses and girders. Rotation in the supports was monitored using tiltmeters. Additionally, the vertical movement in the truss bearings was monitored. Xiao *et al.* (2017) found that the distribution of temperature depends on the daily temperature and sunlight direction. The transverse temperature difference was up to 23°C. The temperature difference between the outside girder and bridge bottom was as high as 23°C. The longitudinal temperature variation was 17°C. Large temperature swings caused thermal expansion that induces bridge's longitudinal movement, bending, and can create torsion. The effect of thermal loading was found to be larger than the effect of traffic loading.

~~~~~  
**21.** The **BR Bridge 1-813** is a steel plate girder with concrete deck composite structure. The bridge was closed due to a 4% tilt in the structure caused by a 50,000 ton pile of dirt on the bridge right of way (McNeil *et al.* 2019). Tiltmeters were installed on 6 concerning piers in order to evaluate the rehabilitation phase. During the construction, temporary post tension members were installed while the bridge was rotated back into place. Strain gauges were placed on these members during the construction phase to observe changes in strain. Post construction, 48 tiltmeters were installed in the structure to continuously monitor any future movement due to settlement (GEOKON 2020).

~~~~~  
**22.** In 2005, the 90 m long **I-64 bridge over US 60** was instrumented for impact detection (Harik and Peiris 2013, Peiris *et al.* 2018). Five strain gauges in the westbound and six in the eastbound direction were installed to either monitor ambient excitation or to evaluate impact damage via strain effects. The impact detection system was completed with infrared sensors to detect trucks exceeding the height limit and then activate an ultrasonic height sensor to determine the truck height and a surveillance camera. A single accelerometer was coupled with a strain gauge to form an impact detector. The program encountered several challenges including continuous power for a bridge in which there was no near by power supply and the need for wired internet, in a time when mobile data communication was not available. While the system was set up successfully, it was never operational due to damage to the data acquisition system that required two replacements, one following vandalism and one following a lightning strike near the power supply unit. The cost of the replacement, as well as the time intervals the system was down, led to decommissioning in 2011.

~~~~~  
**23.** Each of the parallel steel plate-girder **Tennessee River Bridges** consists of nine spans with the main span formed by a steel-girder tied-arch. The effect of thermal movement at the expansion joints was evaluated at five locations, free to move (Peiris *et al.* 2018). Parameters measured included longitudinal expansion/contraction, temperature of the girders and concrete decks, and inclinations of the steel girders in the two approach spans as well as the main span. The instrumentation included also nine LVDTs to measure longitudinal displacements, eleven temperature sensors, and eight tiltmeters. Data loggers were installed at each abutment and the two piers to gather data on displacement, tilt, and temperature.

Peiris *et al.* (2018) showed the structure reactions to short- and long-term temperature variations. Under direct solar radiation, the diurnal temperature difference in the steel girder was

18°C whereas the maximum temperature difference at the bottom of the concrete deck was 9°C. They also reported a series of practical and management issues. Several gauges failed and there were communication errors with the cell modem; as such data could not be gathered continuously for extended periods of time. Due to the fracture critical nature of the bridge, the research team could not drill or weld on to the steel girders in order to attach the gauges. All tiltmeters were adhesively bonded to the girders, and were found to be unreliable. The communication errors were due to failure of the VW analyzer modules utilized to wirelessly communicate between two of the instrumentation locations and the base station housing the data logger and cellular modem. The data acquisition system was not built to store long periods of data onsite. With the bridge being located 400 km away from the researchers, along with lane closures being needed for access to rectify the gauges and communication errors meant large gaps in collected data, it was not possible to quickly remedy problems. Additionally, the expansion joints on either side of the main span were replaced without the research team's knowledge during the monitoring period. Insufficient communication between the researchers and bridge maintenance engineers resulted in a large amount of data loss. The SHM was decommissioned without much success (Peiris *et al.* 2018).

~~~~~  
**24.** The five-span continuous steel girder **I-39 Wisconsin River Bridge** was monitored in July-November 2004 to: (a) perform a fatigue evaluation of various fatigue prone details; (b) estimate the remaining fatigue life of those details; and (c) observe the structural responses under traffic load and under controlled loadings (Mahmoud *et al.* 2005, Liu *et al.* 2009, Orcesi and Frangopol 2011). Twenty-four, weldable and bondable, uniaxial ERSGs were installed on the flanges and the webs of the main girders. Two LVDTs were also installed on two girders to correlate between the stressed measured and the relative displacement between the transverse connection plates and the web of the girders. A data logger was used to collect the data from both the controlled load testing and the long-term monitoring. Mahmoud *et al.* (2005) detailed the layout and the plans of the instrumentation.

Liu *et al.* (2009) presented an approach to assess the bridge system performance through a series-parallel system model consisting of bridge component reliabilities. The correlations among the bridge component safety margins were obtained from field data relative to the Northbound side. Strain was converted into stress under the assumption that the strain data follow the Hooke's law. The work performed by Liu *et al.* (2009) led to several conclusions and the interested readers are referred to the original publication for an extensive discussion about the main outcomes of the study.

~~~~~  
**25.** In early 2000s, the two lane highway **MODOT P-0962 Bridge**, a three-bay monolithic reinforced concrete construction was retrofit with FRP sheets, rods, and wraps to overcome signs of deterioration (Watkins *et al.* 2007). After the rehabilitation, a sensor network was installed (summer 2003) to monitor the central span and measure the load-induced strain in the FRP reinforcement, steel rebar, and the concrete. Extrinsic Fabry-Perot Interferometric (EFPI) strain sensors and ERSGs were installed in the central span in parallel with the reinforcement. Three sets of gauges and sensors, one on the steel rebar, one on the FRP, and one on the surface of the concrete below the roadway surface were used in two locations of the bridge. One set was located on the western longitudinal beam on the mid-span. The other set was placed in the transverse direction of the road deck at mid-span. The sensors located in the deck plate of the structure were mounted to measure transverse strain. Initial testing of the sensors was done with a full-size pick-up truck and static and dynamic loads were recorded. Watkins *et al.* (2007) presented the outcome

of two years monitoring supplemented with a 3D FEM linear elastic analysis of the static load using solid elements (“C3D8”) in ABAQUS. The authors concluded that:

- Fiber optic measurements seemed to show more repeatable results in the longitudinal beam than the transverse deck locations due to better sensitivity to load placement and the environment.
- The EFPI sensors displayed uniform performance in both dynamic and static load tests.
- The EPFI displayed excellent longevity, sensitivity, and accuracy, and overall better operating characteristics than the ERSGs, some of which failed while other were inherently noisier with respect to the EFPI sensors that were more immune to electromagnetic noise.
- The EFPI strains showed general agreement and similar trends with the FEM results.

~~~~~

**26. The C-846 Bridge** is made of four individual structures and 25 spans, with a total length of 1.14 km. The bridge was instrumented with bi- and tri-axial accelerometers in 2001 (Halling and Petty 2001) and an array of twenty-five thermocouples in 2016 (Nichols 2017, Nichols *et al.* 2018). The instrumentation was confined to a single 13 span structure with two expansion joints. The thermocouples were concentrated at a single longitudinal cross section. Nine thermocouples were located through the deck of the left shoulder at approximately 15 inches toward the parapet from the girder. They were embedded in the deck inside a plastic tube full of epoxy. The other thermocouples were located on or near each of the girders. Each girder had a thermocouple next to the top of the girder on the underside of the deck on the concrete, one thermocouple at the top, middle, and bottom of the deck, and one thermocouple next to the bottom of the girder on the bent. Epoxy connected each thermocouple end to the concrete or steel. Nichols (2017) and Nichols *et al.* (2018) studied the correlation between temperature and natural frequencies applying three signal processing to the time history of the ambient vibrations measured with the accelerometers. They found that the higher frequencies have a stronger inverse relationship with the temperature than the lower frequencies.

~~~~~

**27.** A dual-purpose WIM and SHM system was deployed over a single-span 26 m long structure with multiple plate stringers supported by eight girders in Meriden (CT). The structure is herein referred as the **Meriden Bridge**. The system consisted of 38 sensors and 5 different sensing technologies: 18 foil strain gages, 4 piezoelectric strain sensors, 8 piezoelectric accelerometers, 4 accelerometers (with additional temperature sensing capability), and 4 resistance temperature detectors. A study reported by Christenson and Motaref (2016), based on field test conducted with a truck of known-weight passing multiple times, found that: (1) the foil-type strain sensors provided better strain measurements during truck crossings than the piezoelectric strain sensors; (2) both accelerometers provide similar measurements above 3 Hz; (3) the calculated speed, axle spacing and weight data are in reasonable agreement with the measured data.

Jin *et al.* (2015, 2016) combined vibration-based damage detection method and extended Kalman filter-based artificial neural network (EKFNN) to eliminate the temperature effects and detect damage for structures equipped with long-term monitoring systems. They used vibration acceleration and temperature data obtained from the bridge to identify and analyze the correlations between natural frequencies and temperature in order to select proper input variables for the neural network model. A year-long monitoring data were used to train the network. Structural damage scenarios were simulated in a FEM under SAP2000. The damage indicator was the change in the ratios of natural frequency. In testing phase, the damage simulation data of natural frequency time

series were presented to the trained model, and the occurrence of damage was successfully detected by the control limits provided by the damage detection model. The results of the neural network indicate that the EFKNN has better capabilities than benchmark multiple linear regression approach.

An unconventional SHM approach was proposed by Lobo-Aguilar *et al.* (2019) who used infrasound measurements from microphones as a means of noncontact sensing to capture the dynamic properties of the bridge. The empirical measurements were compared to a 3-D FEM created in SAP2000. More recently, Xiao *et al.* (2020) applied video-based tools, the so-called template matching algorithms, along with a subpixel method to collect vision-based structural responses.

~~~~~  
**28.** Seo *et al.* (2013) presented a protocol for the development of load rating distributions for the steel I-girder **US 30 Highway Bridge** in Iowa. The structure is a composite steel–concrete bridge consisting of two travel lanes and three spans with two equal outer spans of 29.7 m and a longer middle span of 38.1 m (Lu *et al.* 2010). Forty FBG-based sensors were distributed in six cross sections to measure strain from five-axle trucks (Wipf *et al.* 2007). The instrumentation layout was designed to monitor the cut-back regions above the north and south floor beam connection plates of a specific section for damage formation. Top flange, web, and bottom flange of girders were monitored to capture the local and global bridge system response. Some sensors were also installed on the deck bottom allowing for the identification of axle number, transverse position, and axle spacing (Seo *et al.* 2013). Each axle of ambient trucks yielded a distinctive peak point for a single deck bottom sensor so that corresponding strains were used to identify ambient truck characteristics. The 40 FOSs were distributed among three individual fiber optic leads, and each fiber was connected to one channel. The strain data were used to calibrate some FEMs created with the software WinGEN. Two scenarios, known and unknown truck characteristic selections, were considered. The studies by Wipf *et al.* (2007) and Phares *et al.* (2007) led to the following main conclusions:

- The installation of the strain gages and laying out the cables required no training or special equipment. Although the time required for sensor installation was only around 30 minutes per gage including surface preparation, securing the sensor cable was relatively labor intensive.
- The live load structural analysis software, BEC Analysis, was deemed accurate.
- During the thirty days monitoring period, the SHM system performed as expected and provided continuous monitoring of the overall performance of the bridge.

~~~~~  
**29.** The **Crum Creek Viaduct** is 274 m long with 17 spans and a steel superstructure with four girder lines carrying two rail tracks, and a substructure comprised of steel columns to create four legged towers (IIS 2020, GEOKON 2020). To address concerns about the superstructure and its remaining fatigue life, and to determine the best methods for rehabilitation, high-speed and VW gages were installed to observe the internal strains in the supporting towers and bents. The measurements were used to determine the load distribution among the substructure as well as monitor changes in stress conditions due to fluctuating temperatures. As part of the preliminary data collection, interpretation and investigation, it was determined that the level of stress in most of the elements was reasonable. After completing a comprehensive geotechnical investigation on the site, it was concluded that slope failure and foundation stability was a concern for this bridge

(IIS 2020).

~~~~~

**30. The Telegraph Road Bridge** is a three-span slab-on-girder highway bridge, completed in 1973. The bridge has been repaired several times, including deck resurfacing in 2011. The original concrete deck had a nominal compressive strength of 20.7 MPa but the new overlay was specified with a 48.3 MPa compressive strength; cylinder tests during the 2011 resurfacing resulted in compressive strengths between 44.1 MPa and 51.0 MPa (Hou *et al.* 2020a, b). A dense network of strain gauges, accelerometers and thermometers was installed, and data were collected daily (Fig. 3). The network was designed to process data in the repository and to extract truck-load events using machine learning. Environmental variations were compensated using nonlinear regression (O'Connor *et al.* 2017). The system was turned on every 2 h to collect data for 1 min with strain, acceleration, and temperature sampled at 100, 200, and 1 Hz, respectively. The first modal frequency of the bridge was estimated to be around 2.5 Hz (O'Connor *et al.* 2017).

Hou *et al.* (2020b) presented the results of 3.5 years monitoring to quantify the composite action in slab-on-girder, and to observe the flexural response of the spans to vehicular loads. The study was complemented with a calibrated analytical model and a FEM both based on field measurements allowing tensile strains in the deck to be estimated under load. The composite action of the bridge was estimated at six different locations. The authors found that the developed partial composite action introduces increased tensile strain in the deck, affecting the durability of the deck itself.

~~~~~

**31. The Carroll Lee Cropper Bridge** is an arch-shaped truss spanning 1235 m. During an inspection, cracks were found along the top of the web in several floor beams. To prevent crack growth, holes were drilled along the crack tips. VW microcrack meters were placed along the cracks and monitored over time to detect any growth. The sensors recorded the maximum and minimum crack openings as well as date and temperature. An allowable crack expansion was determined, and any exceedance of this threshold would immediately alert prominent parties

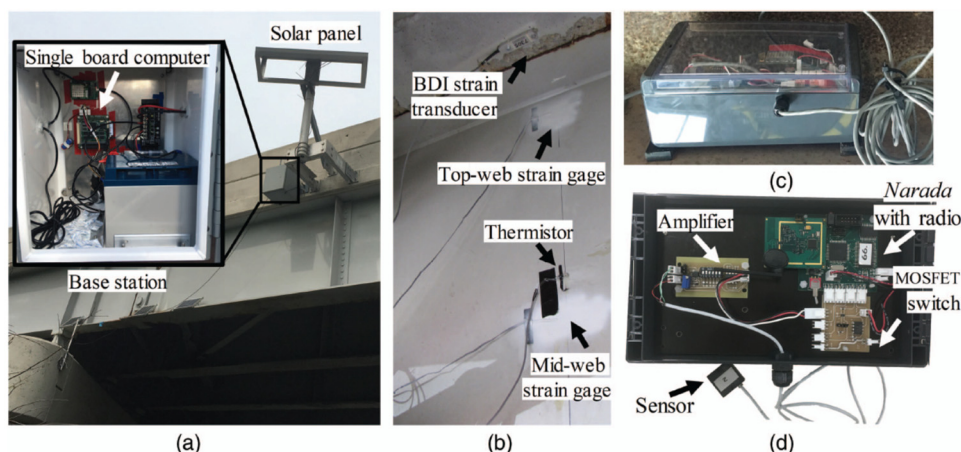


Fig. 3 Highlights of Telegraph Road Bridge instrumentation: (a) base station with solar panel used for power; (b) installation of strain sensors (BDI strain transducer on slab and metal foil gages on girders); (c) wireless sensor enclosure for strain gage data collection magnetically mounted to steel girder flange; and (d) internal components of wireless sensor node. (Figure from Hou *et al.* 2020a)

(Peiris *et al.* 2018).

~~~~~

**32.** The **Huey P. Long bridge** spans 732 m to carry a two-track railroad line with two lanes of vehicular traffic on each side (Weinmann 2015). The bridge was widened to include two new vertical planes of trusses on the outside of the bridge and to add additional lanes and shoulder over the complete four-span river crossing. As part of this expansion project, a truss monitoring system was installed to compare actual versus predicted response of the structure. A system of 769 static and 50 dynamic sensors was used to ensure that the appropriate amount of loads were being transferred from the added beams to the existing beams. Strain gauges evaluated the dead load stresses in existing members, while additional strain gauges measured the live load conditions, and biaxial tiltmeters were installed at each pier. Daily check-ins insured that the structure responded appropriately. Occasionally load tests were completed to calibrate the sensors (Kleinhans 2009).

~~~~~

**33.** The **Tacony-Palmyra Bridge** is a combination steel tied arch and double-leaf bascule bridge, and includes a 168-m steel tied arch span and a 79-m bascule span. The bridge was equipped with a wide variety of sensors and hardware, including VW strain gages to provide measurements on load levels of critical members, seating force of the movable span, and live load force magnitudes. In addition, the expansion and contraction of the arch were measured with crack meters (GEOKON 2020). The data were integrated with videos from a live web portal. The structural monitoring software included the ability to record events such as bascule openings and overloaded vehicle passage. Yarnold *et al.* (2012a, b) used this bridge as a testbed of a temperature-based structural identification technique in which temperature is the forcing function, local strains are another input, and the global displacements are the outputs. The objectives of the evaluation included: (1) FEM calibration, (2) long-term performance, and (3) development of automated alert criteria.

Yarnold and Moon (2015) used the relationship between temperature changes and the consequent strains and displacements to create a graphical baseline of the bridge for SHM purposes. They found that the nonlinear relationship between temperature, local mechanical strains, and global displacements results in a near-flat surface when plotted in 3D space. The bounds and the orientation (angle) of these surfaces were unique for each location and insensitive to normal operational changes in behavior. The numerical results indicated that the surfaces are sensitive to the following three realistic scenarios: (1) bearing failure at the west end; (2) failure of the slotted connection at the east end; (3) failure to the lower chord (downstream side). This latter scenario was considered feasible for several reasons, including stiffness change due to ship impact. A vibration-based baseline was also created and considered to identify the sensitivity to the same three damage scenarios. Changes in natural frequencies and mode shapes (quantified through MAC) of the first eight global modes were considered. Quoting Yarnold and Moon (2015), some conclusions of the study were:

- *The temperature-based 3D surface baseline orientation (angle) and bounds are controlled by the elastic and inelastic properties of the structure, respectively. The surface orientation is defined by the elastic response of the system, thus any changes to elastic properties cause the orientation of the surface to change [...].*
- *[...], localized effects can be identified by changes to the 3D baseline; however, the local measurement component needs to be within the vicinity of the damage location.*
- *The 3D baseline surface has shown to be highly sensitive to realistic damage scenarios [...].*

- A vibration-based baseline [...] was found to be significantly less sensitive for the scenarios examined. The changes in natural frequencies ranged from 0% to 6% with negligible changes to the MAC values.
- The primary drawback of the temperature-based SHM with respect to the vibration-based SHM approach is associated with both implementation time (large temperature swings are required to generate the baseline) and alert time, since certain damage scenarios may also require large temperature swings to diagnose.

~~~~~

**34.** Princeton University opened the pedestrian **Streicker Bridge** in 2010. The structural span extends approximately 107 m. During construction, the bridge was instrumented with discrete FBG sensors and distributed Brillouin Time Domain Analysis sensors. Later, several sensing sheets (Napolitano *et al.* 2019) were added. The sensors measure strain, vibrations, and temperature in the concrete. Glisic (2018) used 7 years of data to gage prestressing force and determine any time-dependent prestress losses due to strand relaxation and concrete creep and shrinkage. The method: (1) uses strain at the centroid of the cross-section as the main parameter to calculate the prestress force, which makes the method robust to the effects of operational load and seasonal variations; (2) accounts for uncertainties, which makes possible probabilistic comparison to code/design estimates; (3) is applicable to wide range of beam-like structures beyond bridge girders. The method aims to overcome the challenges associated with the long-term monitoring of prestress losses, including (1) variable on-site conditions, such as temperature, that affect both the structure and the monitoring system, (2) rheological effects such as creep, shrinkage, and relaxation, that interfere with mechanical effects and affect data analysis, (3) presence of pre-release cracks that affects the distribution of the strain in the structure, (4) inherent uncertainties related to the reliability and accuracy of the monitoring system and (5) inherent uncertain estimation of mechanical and geometrical parameters of concrete. Glisic (2018) concluded that:

- the reliability in identifying both fully functional and problematic sensors was validated; for problematic sensors it was possible to ascertain the type of malfunction;
- the long-term prestress force distribution along the bridge, as well as long-term losses were successfully determined; results showed that although the design and code estimates are generally close to the prestress losses obtained using sensor measurements, they are not necessarily conservative.

Napolitano *et al.* (2019) presented the results about the documentation, organization, and visualization of the metadata associated with the SHM systems employed in the bridge. This management is exemplified in **Fig. 4**. **Fig. 4(a)** shows the capturing interface directed at the sensing sheets under the southeast leg of the bridge. **Fig. 4(b)** shows the same segment of the bridge along with the annotation interface. **Fig. 4(c)** the input of a user who utilizes the point cloud-based annotation, where the dots represent the point cloud and the pink line denotes annotation. Finally, **Fig. 4(d)** shows the annotation not only on the point cloud but also projected back onto the image.

~~~~~

**35.** The Oregon Department of Transportation (ODOT) developed a SHM program to facilitate maintenance and performance monitoring of selected highway bridges. The **Fremont Bridge**, a steel tied-arch bridge, was instrumented to better understand fatigue cracking which is a complicated task as the superstructure has 11,500 horizontal web stiffener terminations inside two arch tie girders (Campbell Scientific 2020b). Eight dataloggers, 64 strain and surface temperatures



Fig. 4 Screen shots of the SHM management system developed for the Streicker Bridge. (a) Example of the initial capture scene; (b) as (a) but with the annotation screen; (c) example of annotation being taken on the point cloud, (d) the annotation projected back onto the image for offsite viewing. (From Napolitano *et al.* 2019)

sensors, and a variety of other sensors were installed to monitor the stress cycles in the tie girders due to thermal loading. According to Campbell Scientific (2020b) ODOT engineers were able to prioritize their retrofitting efforts for the bridge using the data collected from the monitoring system.

~~~~~

**36. The Neville Island Bridge** was the subject of a complete fatigue and fracture evaluation by instrumenting four of its portions: (1) Ramp J, which consists of two-span continuous, two curved steel plate girders; (2) Tied Arch; (3) Span 25 and 26, which are part of four- and two-span continuous units, respectively; straight steel plate girders; (4) Ramp A (Connor *et al.* 2005). The instrumentation consisted of weldable uniaxial resistance strain gages, LVDTs, and accelerometers. The strain gages quantified the stress-range, the LVDTs measured secondary deformations at web gaps, and the accelerometers measured the vibration with the scope of investigating the bridge dynamic properties and assessing the effect that these properties might have on the fatigue performance of the bridge. Controlled load tests using a truck of known weight and geometry and random traffic monitoring were performed. Estimates of the remaining fatigue life were made based on the stress-range histograms determined from the data. Retrofit solutions were recommended for locations where either the predicted life was insufficient, or where cracking has already been observed. The instrumentation was completed by a video camera installed on the tied arch span, and trigger each time a moving vehicle caused the strain to exceed a certain threshold. Kwon and Frangopol (2010) used the data from the bridge to propose a method for fatigue and reliability evaluation and prediction. Probability density functions were used to estimate equivalent stress ranges based on field monitoring data, AASHTO S-N curve was used to provide relevant information about structural details. In this study, Lognormal, Weibull and Gamma distributions were considered. Rain-flow counting method was used to obtain the stress-range bin histogram from the monitoring data. There were seven steps in total to conduct the assessment.

~~~~~

**37.** Kwon and Frangopol (2010) applied the same probabilistic approach mentioned above to a similar structure, the **Birmingham Bridge** (also located in Pittsburgh, PA) using data collected previously (Connor and Fisher 2001). Liang and Chen (2014) proposed and applied a statistical approach for the fatigue life prediction of both the **Neville Island** and the **Birmingham** bridges.

For the for the former, strain data collected during the period between March and April 2004 (Connor *et al.* 2005) were used. For the **Birmingham Bridge** the dynamic data collected from October to November in 2003 (Connor *et al.* 2004) were used. Owing to the scope of this paper, the details of the statistical approach proposed by Liang and Chen (2014) are not given here but the main conclusions were that: (1) the static and dynamic fatigue lives agree reasonably well with the real lives of the bridges and the existing prediction; (2) the Mittag-Leffler distribution is, compared with Lognormal, Gamma and Weibull distributions, the best fit of the stress range data, particularly the peak of the stress range distribution; (3) the proposed modified statistical formula of Miner's rule, which quantifies the relationship between the levels of stress range and the annual traffic increase rate, can reflect the influence of traffic volume increase on the theoretically expected infinite fatigue life of the **Birmingham Bridge**.

~~~~~

**38.** The **Cedar Ave. Bridge**, completed in 1975, is formed by two parallel crossings 1,572 m and 1,580 m long. The bridge was monitored for 22 months (Jan. 2011 – Oct. 2012) with a commercial 16-sensor AE system powered by solar panels to demonstrate that AE technology could be used for global monitoring. The results were presented by Schultz *et al.* (2014) who compared the field data to AE data from fracture laboratory tests of notched cantilever steel beams. The comparison assessed the severity of the AE events recorded in the real bridge. Both field and laboratory data were analyzed using conventional AE parametric analysis. The main conclusion of the study was that the data did not contain evidence of fracture.

~~~~~

**39.** Each of the five spans of the **I-10 Bridge** is made of six lines of pre-fabricated pre-stressed girders, with a cast-on-site superstructure. The girders have a “U” shape cross-section with wings, and were cast over pre-stressed strands in a prefabrication plant, and then steam cured (SMARTEC 2017a). In 2004, 72 SOFO sensors were installed to monitor average normal and shear strain, average curvature, deformed shape and pre-stress losses. The equipment involved all the girders of the fifth span, laying on abutment, with sensors in different configurations. Thermocouples were installed in three cross-sections in order to separate thermally generated strain from structural strain. Other girders were equipped with fewer sensors that are used as control and redundancy. Data analysis was performed using the SOFO VIEW software. The sensors were embedded in the girders during the fabrication. Thus, they provided for full-life measurements of girders, including the very early age and pre-stressing. The system is fully centralized, and measurements are performed automatically from a control room built on-site. According to (SMARTEC 2017a), measurements started immediately after the pouring, the early and very early age deformation were recorded during the first three days, and the deformation was later recorded during the prestress phase, after each strand was cut. Continuous monitoring was also performed before transportation on-site, during transportation and during the pouring of the deck. The results confirmed both the theoretical models as well as the proper health of the bridge post construction.

~~~~~

**40.** The **Columbia River I-5 Bridge** is a steel vertical-lift, “Parker type” through-truss bridge, approximately 1067 m in length with 16 spans. A network of dataloggers, tiltmeters, and laser position sensors monitored the lift span and the counterweights' positions relative to the guide rails. The dataloggers, some of which solar powered, were positioned on the counterweight blocks, on the lift span, and in the operator's control house. Sensor data were collected every five seconds during a bridge opening event, as well as once every four hours to identify trends. Structural performance data was automatically loaded into a database and presented to the bridge engineers

over the computer network (Campbell Scientific 2020c).

~~~~~  
**41.** The **NBI# 00000003231620** bridge consists of a 24.1 cm thick reinforced concrete slab supported by four integral abutment girders with a single-span of 17.07 m. Twenty dual-axis low-cost MEMS accelerometers were used to perform modal testing while eleven strain transducers were used to perform a quasi-static investigation (Whelan *et al.* 2009). Both systems were connected and interfaced with the same wireless hardware consisting of twenty nodes that communicated in a single-network star topology with a central coordinator node connected to a local microcomputer notebook. Responses from ambient loads and vehicular traffic were streamed in real-time from all forty sensor channels distributed across the twenty wireless sensor units. The waveforms were 186 sec long and sampled at 128 Hz. It was determined that the vibration from ambient loading was very small due to the short-span length and the integral abutment design. During the dynamic testing, peak accelerations ranged between 2 and 10 mg. Despite this low excitation, the amplified sensor signals produced clear time-history representations of the traffic loading as well as distinct peaks in the frequency spectra. No signs of phase drifts among the wireless were observed. The main outcome of the study was that the real-time streaming of 40-channels of measurement data sampled at 128 Hz per sensor for ten test durations was successfully achieved while maintaining nearly 100% data delivery across the network. Fourteen mode shapes were extracted (Whelan *et al.* 2009).

~~~~~  
**42.** The 25.91 m long **Nibley Bridge**, completed in 2016, is a single span structure comprised of ten deck bulb girders. During construction, two girders one located on the outer edge and the other located at the center, were instrumented with strain gages, thermocouples, and accelerometers (Alder *et al.* 2018). The initial assessment to determine the natural frequencies was claimed unsuccessful due to issues with noise and digitization. As such, temporary sensors, including L-4C Geophone velocity transducers, were added to perform three tests to calibrate the embedded sensors and identify modal characteristics. One test was an impact and was performed prior to asphalt being placed on the bridge. The other two tests were performed with a vertical shaker after the asphalt was placed prior and after bridge inauguration. The frequencies and modeshapes of the bridge were recorded for each of the three tests with a MAC analysis and compared to analytical mode shapes. The first five modal frequencies were determined. Alder *et al.* (2018) considered also the effect of the temperature and found that some frequencies changed due to the placement of the asphalt and the change in temperature. The additional asphalt lowered all of the detected frequencies.

Pace *et al.* (2019) quantified external loading and resistive prestress. The latter was accomplished by monitoring the long-term changes in prestressing strand strain. Data from eight strain transducers attached to the exterior of the bridge with adhesive and brackets were used. Based on the measured data, bridge traffic regularly exceeded HS-20 truck loading, with recorded strains of up to  $59.26 \mu\epsilon$ . The largest loading events approached the HL-93 design loads. Because the monitoring took place over a narrow timespan, Pace *et al.* (2019) theorized that the maximum strains experienced by the bridge girders could be even higher than the measured values. In addition, the elastic shortening losses were under-predicted, likely due (according to the authors of the report) to an overestimation of the elastic modulus of the concrete. For both the interior and exterior girders, the long-term prestress losses were over-predicted by 31.5% and 11.1%, respectively, using the AASHTO LRFD methods. This over-prediction was attributed to an over-estimate of the creep and shrinkage losses. Overall, Pace *et al.* (2019) found that the girders

immediately under the traffic lanes experienced the highest magnitude of strains. Most of the vehicles (95.62%) caused less than  $5.0 \mu\epsilon$  of strain in any girder. These values reflect smaller vehicles crossing the Nibley Bridge; vehicles smaller than a pickup truck typically caused a strain of  $2.42\text{--}3.45 \mu\epsilon$ . School buses typically caused a strain of around  $13.65 \mu\epsilon$ . Long-term changes in strain were monitored and used to calculate the long-term changes in prestress for an exterior and interior girder. In general, the elastic shortening losses were under-predicted. This was likely due to an overestimation of the elastic modulus of the concrete.

~~~~~  
**43. The New Trammel Creek Bridge** was instrumented with tiltmeters, pressure transducers, and thermocouples. Thermal effects on the substructure were monitored to evaluate stress (Zhu et al. 2015). Pressure cells were placed within the concrete foundations along the piers of the bridge. Tiltmeters were also used along pier caps. Thermocouples were placed along the superstructure to measure ambient temperature. Data collection began in May 2011 and continued at least until the publication of Peiris *et al.* (2018). The field data were supplemented with a FEM and analysis of temperature loadings in order to estimate and compare the bridge pier motion and foundation pressures. Quoting Peiris *et al.* (2018): “*Comparing the FEA-derived pressures generated by introducing extreme temperature values specified in the AASHTO provisions and field data indicates that the AASHTO design provisions produce conservative estimates of foundation design pressures*”.

~~~~~  
**44. The 79 m long double-span Lambert Road Bridge**, built in 1975, carries two traffic lanes by cast-in-place, four-cell, box-girder concrete. Bridge response and environmental conditions were recorded starting May 2011 with 71 sensors: 16 strain gauges, 4 VW strain gauges, 4 velocity transducers (geophones), 3 tiltmeters, and 44 thermocouples. Barr *et al.* (2012) presented the initial live-load and dynamic testing, baseline evaluation, and the long-term monitoring program for the Bridge, including detailed visual inspection, and an NDE deck scan to establish the baseline bridge condition for future comparisons. Foust (2014) studied the relationship between temperature and modal parameters using statistical methods that can distinguish damage from environmental factors. Using information from the tiltmeters and the thermocouples, a relationship between modal frequencies and deck temperature was determined. The study found that natural frequency was affected by changes in temperature only. The peak frequency was shown to be between the peak deck temperature and the peak lower temperature. Statistical regression models were then made between the temperature and the measured frequencies and it was found that there a direct and, in most cases, linear relationship between frequency and temperature (Foust 2014, Foust *et al.* 2014).

~~~~~  
**45. The I-65 bridge** consists of precast prestressed girders supporting a reinforced concrete deck. Cracks were discovered in 95 locations, primarily at fixed end connections which prevented lateral displacement and rotation. CFRP sheets were used to strengthen these regions. LVDTs were installed along two girder lines horizontally and vertically to monitor the retrofit, the growth of existing cracks, or the onset of new cracks (Peiris *et al.* 2018). The LVDTs evaluated conditions both before and after the reinforcement was added and were able to determine if the sheets provided adequate reinforcement or if additional repairs were needed.

~~~~~  
**46. The 47 m long Powder Mill Pond Bridge**, a.k.a. the **Vernon Avenue Bridge** was opened in 2009. It contains 100 strain gauges, 36 girder thermistors, 30 concrete thermistors, 16 bi-axial

tiltmeters, and 16 accelerometers. The strain gauges, temperature sensors, and accelerometers were placed along the N-S pier, and the tiltmeters were located at the N-S abutment. Two 3D FEMs in SAP2000 were created by Santini Bell *et al.* (2010) whereas Sanayei *et al.* (2012), Santini Bell *et al.* (2013) and Kaspar (2018) established a protocol for using strain gauge data to characterize the baseline. The first FEM was created before construction on the basis of design drawings and then calibrated using some load tests. The model made use of solid elements to represent the concrete deck and shell elements for the steel girders. Temperature gradients were also included in the model for calibration purposes. The second FEM was created using BrIM in SAP2000® to form the initial geometry for the bridge. Frame elements were used to represent the girders and support piers. Shells and/or brick elements represented the deck, and spring elements to represent boundary conditions. Sanayei *et al.* (2012) provided further details of the modeling and experimental work related to the static tests on the bridge where it presented the approach for instrumenting the bridge during construction, performing a NDE load test before bridge opening, creating a detailed 3D FEM, calibrating the model using the collected measured strains, and finally, bridge load rating evaluation. Kaspar (2018) analyzed the strain gauges data from 1,929 single-vehicle truck events from 2012 to 2016. Artificial neural network (ANN) and linear regression were developed to identify the relationship between the strains at each of the 27 stations of the bridge. The idea was that the data collected from, let say, 26 locations, would be sufficient to predict the output of the 27<sup>th</sup> location. The algorithms were able to predict the strain at each of the 27 stations with less than 5% average error. The study was completed with a calibrated FEM that simulated three damage scenarios: fascia girder corrosion, girder fracture, and deck delamination. The models trained using the regression and the ANN were able to detect damage in all scenarios with damage being localized in many cases.

~~~~~  
47. The Parker through truss **Rio Puerco Bridge** (Fig. 5) consists of three spans of precast, prestressed I-beams. The bridge was instrumented in 2000 with 64 SOFO sensors to monitor prestress losses, including the early age of the girders (SMARTEC 2017b). Four girders were instrumented with 10 SOFO fiber optic sensors and 6 thermocouples each before pouring and measurements began immediately after pouring. This allowed engineers to determine prestress losses in the girders and real initial strain state of the girders. The results helped to confirm and adjust theoretical models and confirmed the good condition of the bridge after construction.



Fig. 5 Photo of the Rio Puerco Bridge. (From SMARTEC 2017b)

According to SMARTEC (2017b), the long-term monitoring continues to be carried out.

~~~~~  
48. Barr *et al.* (2006) presented the results of a load test performed to determine the load carrying capacity of the **San Ysidro bridge**. Strain gages were attached at the midspan of Span 3 girders. Here, three gages were placed at different elevations: one gage was attached to the bottom flange of the girder to record the largest expected changes in strain; the second and third gages were placed at the bottom and top of the web, respectively. The truck speed was 5–10 mi/hr. to minimize dynamic effects. The field data were compared to a FEM, created using shell and frame elements. Overall, the finite element moment was within 8% of the measured moment when the truck was in the third span of the bridge. The FEM was also used to calculate the load rating for the bridge and these numerical ratings were compared with the load ratings calculated according to the AASHTO standard and LRFD distribution factors. The study lead to the following main conclusions:

- Based on the load ratings using the AASHTO standard and LRFD distribution factors, shear controlled the load rating of the Bridge with an operating rating of 1.2 and 1.11, respectively. However, the finite element results showed that the positive moment on the third span controlled the load rating with an increase in the inventory rating of 4 and 13%, respectively.
- The numerical shear values for the deck were on average 2.8% higher than the measured results.

~~~~~  
49. and 50. The **Horsetail Falls Bridge** and the **Sylvan Bridge** were retrofitted with FRP in 1998 and 2000, respectively, and subsequently instrumented with fiber optics sensors. The monitoring program for the **Horsetail Falls Bridge** was reported in (Soltesz 2002, Kachlakev and McCurry 2000, Kachlakev *et al.* 2001). Twenty-eight sensors monitored the strain, and the data were used to validate a FEM of the bridge. Sixteen sensors were placed at a 45° angle near the end of two beams to monitor the shear strain in the beams. Twelve sensors with a gauge length of 1067 mm were positioned along the main axis at the bottom of those beams to measure flexural strains. Each location had a sensor embedded in the concrete and a sensor attached to the surface of the composite. The composite strengthening increased the capacity of the bridge and the FEM showed that the strain due to a loaded dump truck decreased less than 6% with the FRP strengthening.

Unlike the **Horsetail Falls Bridge**, the **Sylvan Bridge** had several cracks in the beams and exposed to large traffic volumes. Fourteen fiber optics sensors were installed on the same span of the bridge: ten sensors with a gauge length of 100 mm and four with a gauge length of 1000 mm. Nine of the 100-mm sensors were installed as three rosettes in order to measure principal strain and direction. Two rosettes, one 100-mm sensor, and four 1000-mm sensors were positioned on the center beam because it had larger cracks than the other beams. Two rosettes were placed on either side of a crack, and the 100-mm sensor was situated 45° across the crack to monitor the effect of a crack on localized strain fields. The 1000-mm sensors were installed at the beam bottom and just under the bottom of the deck to monitor the neutral axis position. Another rosette was installed on the adjacent beam north of the center beam in the same vicinity from the end of the span and the bottom of the deck. The primary intent of the **Sylvan Bridge** monitoring was to investigate the change in stress field due to FRP strengthening (Soltesz 2002). The data were also used in a computer model of the bridge and for monitoring the bridge response for 3½ years after the composite was installed. Though the data before composite strengthening were not obtained, the one set of measurements summarized in (Soltesz 2002) can be used for comparison to any future testing that may be done on the bridge. The largest strain recorded during the monitoring was 22

$\mu\epsilon$ . As expected, the maximum strain was measured in the flexure zone at the bottom of a beam. Sets of three sensors had been installed on the bridge to create rosettes. The intent was to determine principal strains and directions before and after the composite retrofit. The calculated principal strains and directions, however, varied randomly as a function of time. It was inferred that under static or near-static loading conditions, the rosettes would be effective in determining principal strain and direction, but not under the dynamic load conditions of traffic moving at highway speeds.

~~~~~  
**51. The Kishwaukee River Bridges**, completed in 1980, are twin posttensioned segmental concrete box girder bridges, consisting of five spans 330 m long, with 76.2 m interior spans and 52-m end spans. Strain gages, accelerometers, clip gages and LVDTs were installed (IIS Inc. 2020). A FEM was created and updated using field measurements from a static load test performed in 2000 during which mid-span deflection, axial strains in web closures, average strains, and crack opening in webs were recorded. According to (IIS Inc. 2020), an automated monitoring system for the bridge has been deployed since Dec. 2001 and a few graphs were reported about fatigue crack opening displacement and variation of the 1<sup>st</sup> mode frequency with respect to the temperature. The former was collected for 5 years (2002-2007) whereas the latter refer to 3 years (2004-2006). It is not clear if the system is still active.

~~~~~  
**52. The Watson Wash bridge** is a skewed RC T-girder bridge completed in 1969. Over the years, a combination of increased traffic loads, ASR-related deterioration, and steel reinforcement deficiency had caused significant longitudinal and transverse cracking of the deck soffit (Lee 2005). A forensic study based on initial design documents, inspection reports, and the progression of damage concluded that lack of steel caused the transverse cracks. After a few conventional repairs, the bridge was rehabilitated using external FRP in two critical spans, and details were reported by Lee *et al.* (2007). Modal analysis was conducted on the bridge before and after the FRP-based rehabilitation. The tests were conducted using traffic vibration incorporating an accelerometer grid of six lines of sensors in the longitudinal direction and eleven lines of sensors in the transverse direction. The accelerometers were mounted onto the lower surfaces of the superstructure and the associated time histories were sampled at 200 Hz for a minimum duration of 1 min. The analysis was conducted using time domain decomposition techniques. Four tests were completed: prior and immediately after rehabilitation, 12 months after completion of rehabilitation, and about two years after completion of rehabilitation. To avoid any bias associated with temperature, the tests were performed about the same time of the year. A consistent peak between 5 and 6 Hz was noted in the power spectral density plots. Mode shapes were validated between modal tests using MAC. A 7 to 28% stiffness increase was observed in the rehabilitated locations. Additionally, damage due to ongoing changes could be located and estimated using a simple damage indicator technique.

~~~~~  
**53. The Kings Stormwater Channel Bridge** is a 20-m-long structure consisting of a two-span continuous system with a beam-and-slab superstructure and a five column intermediate pier. The superstructure is composed of six longitudinal filament wound carbon/epoxy circular girders with 9.5 mm wall thickness and a 0.34 m inside diameter pumped full on site with high-slump concrete and connected along their tops to pultruded E-glass/polyester deck panels. Prior to its opening, the bridge was the subject of extensive analytical and experimental characterization. Conventional load tests were conducted prior to and at routine intervals after inauguration (Guan *et al.* 2006).

The dynamic response was characterized through 63 single-axis 0-200 Hz accelerometers, 20 strain gages, 4 linear potentiometers, 1 temperature sensor, and a pantilt-zoom camera. Forty-two out of 63 accelerometers were placed on the bottom of the composite deck to measure vertical acceleration. A horizontal accelerometer was installed in the same equipment housing at some of the nodes, to measure accelerations caused by earthquakes. The strain gages were also attached on the bottom deck, and middle section of the girder. The linear potentiometers were used to measure the deflection of the composite girders at the mid-span of two central girders, which experience the maximum deflection. The overarching goal was to capture the modal characteristics of the bridge and infer the presence of damage by detecting anomalies in the frequency of vibration and mode-shapes.

Guan *et al.* (2007) implemented operational modal analysis algorithms to extract modal parameters from ambient vibrations and a mode shape curvature based damage identification technique in order to localize damage. They also developed a FEM, updated with experimental frequencies. The effect of (simulated) local damage, such as a stiffness change in some of the elements, was shown to have a relatively small impact on global dynamic properties. They found that the change caused by damage is smaller compared to the changes caused by environmental variations, which is detrimental for the practical implementation of modal analysis for bridge SHM.

~~~~~

**54. The I-76 Penncoy Viaduct** was completed in 1952. In 1986, the superstructure was replaced while keeping the original piers and foundations. Displacement measurements were taken using string potentiometers wired to a DAQ system with its own software. Wireless displacement measurements were obtained using an additional set of displacement gauges (identical to the wired string pots) that were transformed into wireless units. These wireless sensors and their transmitters were powered with 9V batteries. Vertical measurements were taken on the first eastbound span using, for comparative purposes, five tethered and five wireless potentiometers. The sensors were attached on the first and the fourth girders of the first eastbound span. The sampling rate was 128 Hz and 100 Hz for the wireless and the wired sensors, respectively. The performance of the wireless sensors was quite satisfactory when compared to their wired counterparts both in the time and frequency domain. The viaduct was also instrumented with wireless magnetic strain gauges. Sold as wired units, these gauges were converted into wireless units by Furkan *et al.* (2020). The performance of these wireless units was compared to VW strain gauges conventionally attached to the structure using epoxy and connected to a separate DAQ system. The wired ERSGs were sampling at 20 Hz, while the wireless strain gauges were sampling at 64 Hz. This comparison showed that wireless data were noisier than the wired data, in part due to the fact that the gauge length of the magnetic gauge was much smaller than the gauge length of the vibrating wire unit, and in part due to the sensing principle (electrical resistance vs vibrating wire frequency). Last but not least, 12 wireless accelerometers were installed after transforming high fidelity wired PCB sensors into wireless units. A direct comparison between wireless and 12 wired units (all sampling at 256 Hz) was conducted by placing the units on four girders on the 1<sup>st</sup> westbound span of viaduct (at  $\frac{1}{4}$ ,  $\frac{1}{2}$  and  $\frac{3}{4}$  span lengths). The mode shapes extracted from the wireless sensing system matched well with their wired counterparts (Furkan *et al.* 2020).

~~~~~

**55. The movable Sunrise Boulevard bridge** was selected to prove a correlation-based SHM methodology to detect and localize structural changes using strain data under operational loading conditions (Catbas *et al.* 2010, 2012). The method tracks the correlation coefficients between strain time histories at different locations. The analysis is framed in **Fig. 6**: strain dynamic data

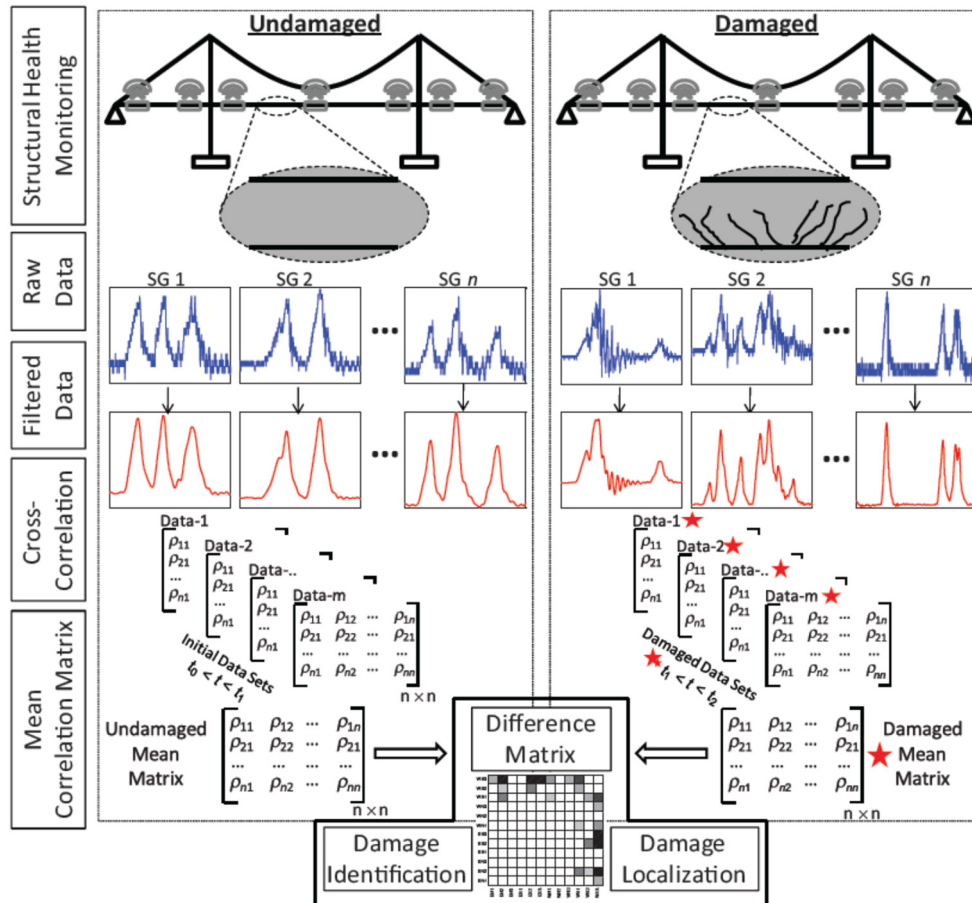


Fig. 6 Overview of the data analysis method proposed by Catbas *et al.* (2012)

relative to the pristine and damaged structure are collected. The dynamic components for each channel are filtered out for the correlation analysis, and the correlation coefficient of each channel is calculated against all the channels to form the correlation matrix for each data set. The procedure is repeated to obtain the correlation matrices throughout the monitoring period and to create a population of matrices from each data set. Finally, set of matrices are averaged for both undamaged and damaged scenarios and their difference matrix is calculated (Catbas *et al.* 2012).

The algorithm was calibrated first in laboratory tests and then validated in the field before, during, and after damage was induced. The results showed that structural changes can be detected and located using the variations in the correlation matrices. The field data also proved the effectiveness of the bridge repair by comparing the bridge performance with respect to undamaged conditions. In the field, an array of 160 sensors monitored main girders, floor beams, stringers, live load shoes (LLSs), and span locks (SLs). On a movable bridge, LLSs are the support locations of the main girders in closed position and are one of the critical structural components. Main operational concern of LLS is the loss of contact that makes the shims crucial at these locations. Small gaps due to deterioration of the shims lead the girders to pound on the LLSs, which results in further misalignment, additional stresses, stress redistributions, fatigue damage, and excessive

wear (Catbas *et al.* 2012). Data from the dynamic strain gages at the bottom flanges of the main girders were sampled at 250 Hz. Damage was induced by removing both LLS and SL shims to mimic common structural maintenance problems related with LLS and SL shims removal. First, the West South LLS (WS3) shims were removed (Case 1), then the West South SL (WS1) shims (Case 2), and finally, the shims from LLS and SL of West South side were removed for the combined damage scenario (Case 3). The concept presented in **Fig. 6** was applied to the bridge data under pristine conditions, when the three damage cases were induced (Cases 1–3), and after damage was repaired. Then, the difference matrices were obtained for each case. Ten different data sets were collected for the baseline case (pristine conditions). Five data sets were collected for each damage case (Cases 1–3). Afterward, the shims were replaced, and ten new data sets were collected. All the collections occurred during normal operating traffic, and no special trucks or lane closures were required. Catbas *et al.* (2012) successfully correlated the strain time histories from different sensor locations to damaged conditions. The cross-correlations of the strain indicated a level of correlation among different sensor pairs. The correlation analysis reduced the data size to provide useful information from large amounts of data, thus offering an efficient data handling capability. According to the authors of the research, the proposed approach eliminates the need for loading information (magnitude and placement) for strain monitoring applications because the strain time histories were obtained from arbitrary operating traffic conditions. If the correlation was not employed, raw strain data may have led to false negatives/positives since the strain levels depends on the traffic.

Catbas and Malekzadeh (2016) expanded previous works by presenting a machine learning algorithm to process the data collected from the mechanical components of the bridge. The algorithm was trained by extracting statistical features and conducting cross correlation analysis and robust regression analysis, using 4 years of field data. The collected data were utilized to assess the performance of the algorithm under baseline and different common damage scenarios. The system had a satisfactory performance for the detection of the damage scenarios caused by leakage and lack of sufficient oil in gearbox, as well as bolt removal from rack and pinion.

~~~~~

SENSR Monitoring Technologies, LLC. investigated a few Canadian and U.S. rail bridges using a hybrid sensor that measures acceleration, tilt, and temperature in order to detect scour and changing soil conditions (Orsak 2019). The U.S. bridges were the **BNSF Bridge 77.54** (Nodaway, MO), the **BNSF Bridge 279.7** (Gorin, MO), the **CPR Bridge 195.20** (Tomah, WI), and the **CPR 121.95 Watertown** near Ixonia (WI). The sensors had been in operation from 2013 to 2017 to monitor: average tilt, dynamic tilt (along two directions), and acceleration. The first feature was adjusted for temperature and best used when the bridge was unloaded. The other two were recorded during train loading. The sensors continuously stored data and transmitted them to an onsite DAQ unit, branded “SENSRnet.” Information about the temperature was collected as well. The following main observations and recommendations were made (Orsak 2019) regarding the bridges in the U.S.:

- Piers 2, 4, and 5 of the **Bridge 77.54** should continue to be monitored for signs of scour. The data have shown changes in response that warrant continued monitoring efforts. Given the scour history of Pier 2, an underwater inspection may be necessary. Pier 3 has shown no alarming data.
- The tilt of a pier of the **Bridge 279.7** shifted over  $0.05^\circ$  and should be monitored in the future.

- The sensors mounted on the steel structural members of the CPR Bridge 195.20 show highly variable and difficult-to-use data. It is recommended to focus future monitoring efforts on sensors mounted directly on concrete or masonry elements. The sensor mounted on the bridge pier has reported consistent tilt and vibration data indicative of stable conditions.
- The West abutment of the CPR 121.95 Bridge shifted over 0.15 degrees since monitoring began in 2013 and further monitoring is recommended.

## 5. Conclusions

This paper reviewed the instrumentation programs for bridge health monitoring applications in the U.S. Based on the scientific literature retrieved during this review, over sixty bridges were found to have been instrumented for monitoring static and/or dynamic responses. This review focused primarily on the three topics: (1) methodologies and objectives of the bridge instrumentation programs; (2) data inference methods to evaluate structural parameters and detect structural irregularities; (3) data validation techniques. The documents analyzed and reviewed were published after year 2000 with some of them as old as a few months. Most of the documents were authored by researchers from the academia and only a small fraction came directly from companies financially involved with the instrumentation installed. Most of the researches was funded by state transportation agencies and in a lower measure by federal grants. According to the information collected during this review, the following conclusions can be drawn:

- (1) Most of the bridge instrumentation programs included at least three different sensors types: one to collect ambient conditions (e.g., temperature and wind); one to collect static performance (e.g., strain gages); one to collect dynamic responses (e.g., accelerometers).
- (2) The vast majority of the monitored bridges less than 30 years old at the time the monitoring began. A few bridges were instrumented during construction.
- (3) Strain gages are, by far, the most common instrumentation used.
- (4) While conventional foil strain gages, i.e., ERSGs, were extensively used in old programs, in recent years there has been an increasing interest in fiber optic technology, which is also gaining momentum as fiber optics may integrate multiple sensing modalities using robust and rugged technology.
- (5) A good number of publications report short-term monitoring, which refers to a few controlled load truck tests.
- (6) Long-term monitoring programs are in most cases continuous observations conducted over a few months period and in a few cases a few years period.
- (7) Time-series associated with the dynamic response of bridge are almost always converted into the frequency domain in order to extract the frequency of vibration of as many modes as possible and use them as indicator of potential damage.
- (8) There is a general well-established consensus that temperature plays a detrimental role in the modal analysis of bridges and any robust SHM strategy cannot disregard the effect of temperature on mode shapes and vibration frequencies in order to avoid false positives/negatives. To this end, there have been numerous researches, not examined in the context of this review article, that aim at addressing the adverse effect of normal fluctuations in the environment on the effectiveness of damage detection techniques (e.g., Sen *et al.* 2019).

- (9) Factors such as snow or water seems to have been persistently neglected as potential factors influencing the field data.
- (10) Wireless sensors are gaining momentum in bridge health monitoring. However, there are still technical challenges that prevent their exclusive use in lieu of conventional wired systems.
- (11) Owing to the size of the structures being involved and owing to the nature of the degradation processes, robust finite element modeling seems to be the preferred way to validate any SHM protocol installed in a given bridge. For some of the bridges discussed in this review, 3D FEM were implemented using commercial software such as ABAQUS or SAP2000.
- (12) Whenever finite element modeling has supplemented the SHM protocols, the latter ones are deemed the ones providing the accurate results and therefore the models are calibrated to “match” field data.
- (13) Based on conclusion in bullet 12, researchers have come to the conclusion that field measurements are reliable and initial models are not accurate enough to portray the effective response the structure to real loads and traffic. So, calibration is always warranted.
- (14) Only a few studies have reported inaccuracies of sensors data. Most of the issues reported was related to vandalism, power supplies, and maintenance. It is believed of the authors of this review that any issue associated with the sensors that invalidated data would not be reported in the published documents. As such, it is difficult to gage the success rate and the durability of the instrumentation programs presented here.
- (15) As bridges have very little in common with each other and almost any new bridge is unique, it is difficult to design a uniform SHM paradigm valid for any bridge. What is adequate for some may not be adequate for another. This complication increases when structures are modeled but damage can only be simulated numerically and not (logically) induced experimentally.
- (16) Following bullet 15, it is not guarantee that a damage identification method developed for a certain bridge is applicable to another bridge. As demonstrated in a few studies (e.g., Talebinejad *et al.* 2011) some methods work and some methods do not even work for a given bridge using the same data set.
- (17) A follow-up to bullet 15, only one study reported the use of a SHM strategy for two bridges, which are considered “sisters”: the Neville Island Bridge and the Birmingham Bridge.
- (18) In only one study, the bridge under consideration was “physically damaged” and repaired to consent the observation of the system prior, during, and after a structural flaw.

Future studies shall aiming at collecting a more comprehensive portray of the state-of-the-art in bridge health monitoring in the U.S. or elsewhere, shall focus on the preparation and distribution of a detailed online survey to be sent to all state DOTs and rail owners (if in the U.S.) or agencies responsible of the management of this strategically important civil engineering structures.

## Acknowledgments

The authors acknowledge the support of the Pennsylvania Department of Transportation (PennDOT) under the Work Order-003 titled “Data Management, Mining, and Inference for

Bridge Monitoring”. The initial contribution of Dr. Max Stephens and Miss Qianyun (Gloria) Zhang is acknowledged. The use of the results or reliance on the material presented is the responsibility of the reader. The contents of this document are not meant to represent standards and are not intended for use as a reference in specifications, contracts, regulations, statutes, or any other legal document. The opinions and interpretations expressed are those of the authors and other duly referenced sources. The views and findings reported herein are solely those of the writers and not necessarily those of PennDOT. This paper does not constitute a standard, a specification, or regulations.

## References

- Adams, D. (2007), *Health Monitoring of Structural Materials and Components: Methods with Applications*, John Wiley & Sons.
- Agdas, D., Rice, J.A., Martinez, J.R. and Lasa, I.R. (2015), “Comparison of visual inspection and structural-health monitoring as bridge condition assessment methods”, *J. Perform. Constr. Facil.*, **30**(3), 04015049.
- Ahlborn, T.M., Shuchman, R., Sutter, L.L., Brooks, C.N., Harris, D.K., Burns, J.W., Endsley, K.A., Evans, D.C., Vaghefi, K. and Oats, R.C. (2010), “The state-of-the-practice of modern structural health monitoring for bridges: A comprehensive review”, Technical Report for Contract No. DTOS59-10-H-00001; Michigan Technological University, MI, USA. <https://trid.trb.org/view/1101239>
- Aktan, A.E., Catbas, F.N., Grimmelsman, K.A. and Pervizpour, M. (2002), “Development of a model health monitoring guide for major bridges”, Technical Report for Contract No. DTFH61-01-P-00347; Federal Highway Administration Research, Development and Drexel intelligent infrastructure and transportation safety institute, pp. 183-230.
- Alder, T.S., Halling, M.W. and Barr, P.J. (2018), “Installation of embedded accelerometers in precast girders for the Nibley Utah Bridge”, Report No. CAIT-UTC-NC34; Rutgers University, Bridge Diagnostic Instruments, U.S. Department of Transportation Federal Highway Administration.
- Al-Khateeb, H.T., Shenton III, H.W., Chajes, M.J. and Aloupis, C. (2019), “Structural health monitoring of a cable-stayed bridge using regularly conducted diagnostic load tests”, *Front. Built Environ.*, **5**(41). <https://doi.org/10.3389/fbuil.2019.00041>
- Aono, K., Hasni H., Pochettino O., Lajnef, N. and Chakrabartty, S. (2019), “Quasi-self-powered piezo-floating-gate sensing technology for continuous monitoring of large-scale bridges”, *Front. Built Environ.*, **5**(29). <https://doi.org/10.3389/fbuil.2019.00029>
- Babanajad, S., Moon, F., Braley, J., Ansari, F., Norouzzadeh, E., Taylor, T., Roy, S. and Maher, A. (2020), “Structural health monitoring of representative cracks in the Manhattan bridge”, Report No. CAIT-UTC-NC61; Rutgers University, New York City (NYC), Department of Transportation.
- Barr, P.J., Woodward, C.B., Najera, B. and Amin, M.N. (2006), “Long-term structural health monitoring of the San Ysidro Bridge”, *J. Perform. Constr. Facil.*, **20**(1), 14-20. [https://doi.org/10.1061/\(ASCE\)0887-3828\(2006\)20:1\(14\)](https://doi.org/10.1061/(ASCE)0887-3828(2006)20:1(14))
- Barr, P.J., Petroff, S.M., Hodson, D.J., Thurgood, T.P. and Halling, M.W. (2012), “Baseline testing and long-term monitoring of the Lambert Road Bridge for the long-term bridge performance program”, *J. Civil Struct. Health Monitor.*, **2**(2), 123-135. <https://doi.org/10.1007/s13349-012-0023-2>
- Betti, R., Khazem, D., Carlos, M., Gostautas, R. and Virmani, Y. (2014), “Corrosion monitoring research for city of New York bridges”, Report No. FHWA-HRT-14-023; U.S. Department of Transportation.
- Betti, R., Sloane, M.J.D., Khazem, D. and Gatti, C. (2016), “Monitoring the structural health of main cables of suspension bridges”, *J. Civ. Struct. Health Monitor.*, **6**(3), 355-363. <https://doi.org/10.1007/s13349-016-0165-8>
- Campbell Scientific (2020a), Delaware River: Bridge Health - Campbell gear used in structural-health monitoring system for the Burlington-Bristol Bridge, Campbell Scientific, Inc., Logan, USA. [www.campbellsci.com/delaware-river-bridge](http://www.campbellsci.com/delaware-river-bridge)

- Campbell Scientific (2020b), Oregon: Monitoring Bridge Stress and Strain - Campbell Scientific system monitors thermal loading effects on bridge tie girders, Campbell Scientific, Inc., Logan, USA. [www.campbellsci.com/fremont-bridge](http://www.campbellsci.com/fremont-bridge)
- Campbell Scientific (2020c), Oregon: Bridge Lift Span Performance - Campbell CR1000 dataloggers monitor lift span and counterweight system, Campbell Scientific, Inc., Logan, USA. [www.campbellsci.com/i5-bridge](http://www.campbellsci.com/i5-bridge)
- CANARY Systems (2020), [https://canarysystems.com/pdfs/canary\\_pp20.pdf](https://canarysystems.com/pdfs/canary_pp20.pdf)
- Catbas, F.N. and Malekzadeh, M. (2016), “A machine learning-based algorithm for processing massive data collected from the mechanical components of movable bridges”, *Autom. Constr.*, **72**(3), 269-278. <https://doi.org/10.1016/j.autcon.2016.02.008>
- , F.N., Susoy, M. and Frangopol, D.M. (2008), “Structural health monitoring and reliability estimation: Long span truss bridge application with environmental monitoring data”, *Eng. Struct.*, **30**(9), 2347-2359. <https://doi.org/10.1016/j.engstruct.2008.01.013>
- Catbas, F.N., Gul, M., Zaurin, R., Gokce, H.B., Terrell, T., Dumlupinar, T. and Maier, D. (2010), “Long term bridge maintenance monitoring demonstration on a movable bridge: A framework for structural health monitoring of movable bridges”, Technical Report for Contract No. BD548-23; University of Central Florida, Orlando, FL, USA. <https://trid.trb.org/view/927119>
- Catbas, F.N., Gokce, H.B. and Gul, M. (2012), “Nonparametric analysis of structural health monitoring data for identification and localization of changes: Concept, lab, and real-life studies”, *Struct. Health Monitor.*, **11**(5), 613-626. <https://doi.org/10.1177/1475921712451955>
- Cawley, P. (2018), “Structural health monitoring: Closing the gap between research and industrial deployment”, *Struct. Health Monitor.*, **17**(5), 1225-1244. <https://doi.org/10.1177/1475921717750047>
- Chang, M. and Pakzad, S.N. (2013), “Modified natural excitation technique for stochastic modal identification”, *J. Struct. Eng.*, **139**(10), 1753-1762. [https://doi.org/10.1061/\(ASCE\)ST.1943-541X.0000559](https://doi.org/10.1061/(ASCE)ST.1943-541X.0000559)
- Chang, M., Pakzad, S.N. and Schanck, C. (2011), “Framework for comparison study of stochastic modal identification considering accuracy and efficiency”, *Struct. Health Monitor.*
- Chen, G., Yan, D., Wang, W., Zheng, M., Ge, L. and Liu, F. (2007), “Assessment of the Bill Emerson memorial cable-stayed bridge based on seismic instrumentation data”, Technical Report No. OR08-003; Center for Infrastructure, Missouri University of Science and Technology, Rolla, MO, USA. [https://scholarsmine.mst.edu/civarc\\_enveng\\_facwork/957/](https://scholarsmine.mst.edu/civarc_enveng_facwork/957/)
- Chen, J.G., Adams, T.M., Sun, H., Bell, E.S. and Büyükoztürk, O. (2018), “Camera-based vibration measurement of the world war I memorial bridge in Portsmouth, New Hampshire”, *J. Struct. Eng.*, **144**(11), 04018207. [https://doi.org/10.1061/\(ASCE\)ST.1943-541X.0002203](https://doi.org/10.1061/(ASCE)ST.1943-541X.0002203)
- Connor, R.J. and Fisher, J.W. (2001), “Report on Field Inspection, Assessment, and Analysis of Floorbeam Connection Cracking on the Birmingham Bridge-Pittsburgh PA”, Report No. 02-10; Lehigh University, Bethlehem, PA, USA.
- Connor, R.J., Fisher, J.W., Hodgson, I.C. and Bowman, C.A. (2004), “Results of field monitoring prototype floorbeam connection retrofit details on the Birmingham Bridge”, Report No. 04-04; Lehigh University, Bethlehem, PA, USA.
- Connor, R.J., Hodgson, I.C., Mahmoud, H. and Bowman, C. (2005), “Field Testing and Fatigue Evaluation of the I-79 Bridge over the Ohio River”, Report No. 05-02; Lehigh University, Bethlehem, PA, USA.
- Conte, J., He, X., Moaveni, B., Masri, S.F., Caffrey, J.P., Wahbeh, M., Tasbihgoo, F., Whang, D.H. and Elgamal, A. (2008), “Dynamic testing of Alfred Zampa memorial bridge”, *J. Struct. Eng.*, **134**(6), 1006-1015. [https://doi.org/10.1061/\(ASCE\)0733-9445\(2008\)134:6\(1006\)](https://doi.org/10.1061/(ASCE)0733-9445(2008)134:6(1006))
- Christenson, R.E. and Motaref, S. (2016), “Dual Purpose Bridge Health Monitoring and Weigh-in-Motion (BWIM): Phase I”, Report No. CT-2265-F-15-7; University of Connecticut, Mansfield, CT, USA.
- Dalia, Z.M., Bagchi, S., Sabamehr, A., Bagchi, A. and Bhowmick, A. (2018), “Life cycle cost-benefit analysis of SHM of I-35 W St. Anthony Falls bridge”, In: *International Symposium on Structural Health Monitoring and Nondestructive Testing*, Saarbruecken, Germany, October.
- De Roeck, G., Degrande, G., Lombaert, G. and Müller, G. (2011), “Examples of Vibration-Based Bridge

- Structural-Identification for Management”, *Proceedings of the 8th International Conference on Structural Dynamics, EURO-DYN 2011*, Leuven, Belgium, July.
- Dong, Y., Song, R. and Liu, H. (2010), “Bridges Structural Health Monitoring and Deterioration Detection-Synthesis of Knowledge and Technology”, Report No. 309036; Alaska Department of Transportation and Public Facilities, University of Alaska, Fairbanks, AK, USA.
- Faridazar, F. (2019), “Toward Self-Diagnosing Bridges”, *Public Roads*, **82**(4).
- Farrar, C.R. and Worden, K. (2007), “An introduction to structural health monitoring”, *Phil. Trans. R. Soc. A.*, **365**, 303-315. <https://doi.org/10.1098/rsta.2006.1928>
- Farrar, C.R. and Worden, K. (2012), *Structural Health Monitoring: A Machine Learning Perspective*, John Wiley & Sons.
- Federal Highway Administration (2019a), <https://www.fhwa.dot.gov/bridge/nbi/ascii.cfm>
- Federal Highway Administration (2019b), <https://www.fhwa.dot.gov/bridge/britab.cfm#def>
- Federal Highway Administration (2019c), <https://www.fhwa.dot.gov/bridge/fc.cfm>
- Feng, M.Q. (2019), “A Novel Vision Sensor for Remote Measurement of Bridge Displacement”, Report No. NCHRP IDEA Project 189; Columbia University, New York, NY, USA.
- Feng, D. and Feng, M.Q. (2017), “Experimental validation of cost-effective vision-based structural health monitoring”, *Mech. Syst. Signal Process.*, **88**, 199-211. <https://doi.org/10.1016/j.ymssp.2016.11.021>
- Foust, N. (2014), “Statistical Models of the Lambert Road Bridge: Changes in Natural Frequencies due to Temperature”, Master of Science Thesis; Utah State University, Logan, UT, USA.
- Foust, N.R., Halling, M.W. and Barr, P.J. (2014), “Statistical models of a concrete bridge: changes in modal parameters due to temperature”, In: *Structures Congress*, Boston, MA, USA, April. <https://doi.org/10.1061/9780784413357.184>
- French, C.E., Hedegaard, B., Shield, C.K. and Stolarski, H. (2011), “I35W Collapse, Rebuild, and Structural Health Monitoring — Challenges Associated with Structural Health Monitoring of Bridge Systems”, *Proceedings of the 18th International Conference on Positron Annihilation*, FL, USA, August.
- French, C.E.W., Shield, C.K., Stolarski, H.K., Hedegaard, B.D. and Jilk, B.J. (2012), “Instrumentation, Monitoring, and Modeling of the I-35W Bridge”, Report No. MN/RC 2012-24; Minnesota Department of Transportation, Minneapolis, MN, USA.
- French, C.E.W., Shield, C.K. and Hedegaard, B.D. (2014), “Modeling and monitoring the long-term behavior of post-tensioned concrete bridges”, Report No. MN/RC 2014-39; Minnesota Department of Transportation, Minneapolis, MN, USA.
- Furkan, M.O., Mao, Q., Livadiotis, S., Mazzotti, M., Aktan, A.E., Sumitro, S.P. and Bartoli, I. (2020), “Towards rapid and robust measurements of highway structures deformation using a wireless sensing system derived from wired sensors”, *J. Civil Struct. Health Monitor.*, **10**, 297-311. <https://doi.org/10.1007/s13349-020-00385-5>
- Gaebler, K.O., Hedegaard, B.D., Shield, C.K. and Linderman, L.E. (2018), “Signal selection and analysis methodology of long-term vibration data from the I-35W St. Anthony Falls Bridge”, *Struct. Control Health Monitor.*, **25**(7), e2182. <https://doi.org/10.1002/stc.2182>
- GEOKON (2020), Bridges, New Hampshire, USA. <https://www.geokon.com/Bridges>
- Glisic, B. (2018), “Long-term evaluation of prestress losses in concrete bridges using long-gauge fiber optic sensors”, Report No. CAIT-UTC-NC-48; Princeton University, Princeton, NJ, USA.
- Guan, H., Karbhari, V.M. and Sikorsky, C.S. (2006), “Web-based structural health monitoring of an FRP composite bridge”, *Computer-Aided Civil Infrastruct. Eng.*, **21**(1), 39-56. <https://doi.org/10.1111/j.1467-8667.2005.00415.x>
- Guan, H., Karbhari, V.M. and Sikorsky, C.S. (2007), “Long-term structural health monitoring system for a FRP composite highway bridge structure”, *J. Intell. Mate. Syst. Struct.*, **18**(8), 809-823. <https://doi.org/10.1177/1045389X06073471>
- Guo, T. and Chen, Y.W. (2011), “Field stress/displacement monitoring and fatigue reliability assessment of retrofitted steel bridge details”, *Eng. Fail. Anal.*, **18**(1), 354-363. <https://doi.org/10.1016/j.engfailanal.2010.09.014>
- Guo, T., Frangopol, D.M. and Chen, Y. (2012), “Fatigue reliability assessment of steel bridge details

- integrating weigh-in-motion data and probabilistic finite element analysis”, *Comput. Struct.*, **112**, 245-257. <https://doi.org/10.1016/j.compstruc.2012.09.002>
- Halling, M.W. and Petty, T. (2001), “Strong Motion Instrumentation of I-15 Bridge C-846”, Report No. UT-01-12; Research and Development Division, The Utah Department of Transportation, Taylorsville, UT, USA.
- Harik, I. and Peiris, A. (2013), “Case Studies of Structural Health Monitoring of Bridges”, In: *Nondestructive Testing of Materials and Structures*, RILEM Bookseries, **6**, 1007-1013, Springer, Dordrecht, Netherlands.
- Hartnagel, B.A., O’Connor, J., Yen, W.H., Clogston, P. and Çelebi, M. (2006), “Planning and implementation of a seismic monitoring system for the Bill Emerson Memorial Bridge in Cape Girardeau, MO”, *Proceedings of Structures Congress 2006: Structural Engineering and Public Safety*, St. Louis, MO, USA, May.
- He, X., Moaveni, B., Conte, J.P., Elgamal, A. and Masri, S.F. (2008), “Modal identification study of Vincent Thomas Bridge using simulated wind-induced ambient vibration data”, *Computer-Aided Civil Infrastruct. Eng.*, **23**(5), 373-388. <https://doi.org/10.1111/j.1467-8667.2008.00544.x>
- He, X., Moaveni, B., Conte, J.P., Elgamal, A. and Masri, S.F. (2009), “System identification of Alfred Zampa Memorial Bridge using dynamic field test data”, *J. Struct. Eng.*, **135**(1), 54-66. [https://doi.org/10.1061/\(ASCE\)0733-9445\(2009\)135:1\(54\)](https://doi.org/10.1061/(ASCE)0733-9445(2009)135:1(54))
- Hedegaard, B.D., French, C.E., Shield, C.K., Stolarski, H.K. and Jilk, B.J. (2013), “Instrumentation and modeling of I-35W St. Anthony Falls bridge”, *J. Bridge Eng.*, **18**(6), 476-485. [https://doi.org/10.1061/\(ASCE\)BE.1943-5592.0000384](https://doi.org/10.1061/(ASCE)BE.1943-5592.0000384)
- Hedegaard, B.D., French, C.E. and Shield, C.K. (2017a), “Time-dependent monitoring and modeling of I-35W St. Anthony Falls Bridge. I: Analysis of monitoring data”, *J. Bridge Eng.*, **22**(7), 04017025. [https://doi.org/10.1061/\(ASCE\)BE.1943-5592.0001053](https://doi.org/10.1061/(ASCE)BE.1943-5592.0001053)
- Hedegaard, B.D., French, C.E. and Shield, C.K. (2017b), “Long-term monitoring strategy for time-dependent deflections of posttensioned concrete bridges”, *J. Bridge Eng.*, **22**(11), 04017095. [https://doi.org/10.1061/\(ASCE\)BE.1943-5592.0001139](https://doi.org/10.1061/(ASCE)BE.1943-5592.0001139)
- Helmicki, A. and Hunt, V. (2013), “Instrumentation of the US grant bridge for monitoring of fabrication, erection, in-service behavior, and to support management, maintenance, and inspection”, Report No. FHWA/OH-2013/23; Office of Statewide Planning and Research, The Ohio Department of Transportation, Columbus, OH, USA.
- Hong, A.L., Ubertini, F. and Betti, R. (2011), “Wind analysis of a suspension bridge: Identification and finite element model simulation”, *J. Struct. Eng.*, **137**(1), 133-142. [https://doi.org/10.1061/\(ASCE\)ST.1943-541X.0000279](https://doi.org/10.1061/(ASCE)ST.1943-541X.0000279)
- Hooks, J.M. and Weidner, J. (2016), “Long-Term Bridge Performance Program Protocols, Version 1”, Report No. FHWA-HRT-16-007; Office of Infrastructure Research and Development, Turner-Fairbank Highway Research Center, McLean, VA, USA.
- Hou, R., Jeong, S., Lynch, J.P. and Law, K.H. (2020a), “Cyber-physical system architecture for automating the mapping of truck loads to bridge behavior using computer vision in connected highway corridors”, *Transp. Res. Part C: Emerg. Technol.*, **111**, 547-571. <https://doi.org/10.1016/j.trc.2019.11.024>
- Hou, R., Lynch, J.P., Ettouney, M.M. and Jansson, P.O. (2020b), “Partial composite-action and durability assessment of slab-on-girder highway bridge decks in negative bending using long-term structural monitoring data”, *J. Eng. Mech.*, **146**(4), 04020010. [https://doi.org/10.1061/\(ASCE\)EM.1943-7889.0001725](https://doi.org/10.1061/(ASCE)EM.1943-7889.0001725)
- Hunt, B.E. (2009), *Monitoring Scour Critical Bridges*, National Academies of Sciences, Engineering, and Medicine, Washington, DC, USA.
- IIS (2020), <https://www.iisengineering.com/projects/structural-health-monitoring-of-septas-crum-creek-viaduct/>
- IIS Inc. (2020), [http://www.iis-system.com/media/Applications\\$20SHM.pdf](http://www.iis-system.com/media/Applications$20SHM.pdf)
- Inaudi, D., Bolster, M., Deblois, R., French, C., Phipps, A., Sebasky, J. and Western, K. (2009), “Structural health monitoring system for the new I-35W St Anthony Falls Bridge”, *Proceedings of the 4th*

- International Conference on Structural Health Monitoring of Intelligent Infrastructure (SHMII-4)*, Zurich, Switzerland, July.
- Kachlakev, D.I. and McCurry, D.D. (2000), “Testing of Full-Size Reinforced Concrete Beams Strengthened with FRP Composites: Experimental Results and Design Methods Verification”, Report No. FHWA-ORRD-00-19; Oregon Department of Transportation and Federal Highway Administration, OR, USA.
- Kachlakev, D.I., Miller, T., Yim, S., Chansawat, K. and Potisuk, T. (2001), “Finite Element Modeling of Concrete Structures Strengthened with FRP Laminates”, Report No. FHWA-OR-RD-01-17; Oregon Department of Transportation and Federal Highway Administration, OR, USA.
- Karbhari, V.M. and Ansari, F. (2009), *Structural Health Monitoring of Civil Infrastructure Systems*, Woodhead Publishing, Elsevier.
- Kaspar, K.E. (2018), “A Protocol for Using Long-Term Structural Health Monitoring Data to Detect and Localize Damage in Bridges”, Master of Science Theses, University of New Hampshire, Durham, England.
- Khuc, T. and Catbas, F.N. (2018), “Structural identification using computer vision-based bridge health monitoring”, *J. Struct. Eng.*, **144**(2), 04017202. [https://doi.org/10.1061/\(ASCE\)ST.1943-541X.0001925](https://doi.org/10.1061/(ASCE)ST.1943-541X.0001925)
- Kleinhaus, D.D. (2009), “Structural Monitoring for the Huey P. Long Bridge Widening Project”, *AREMA 2009 Annual Conference & Exposition*, Chicago, Illinois, September.  
[https://www.arena.org/files/library/2009\\_Conference\\_Proceedings/Structural\\_Monitoring\\_for\\_The\\_Huey\\_P\\_Long\\_Bridge\\_Widening\\_Project.pdf](https://www.arena.org/files/library/2009_Conference_Proceedings/Structural_Monitoring_for_The_Huey_P_Long_Bridge_Widening_Project.pdf)
- Kulcu, E., Qin, X., Barrish, R. and Aktan, A. (2000), “Information technology and data management issues for health monitoring of the Commodore Barry Bridge”, *Proceedings of SPIE’s 5th Annual International Symposium on Nondestructive Evaluation and Health Monitoring of Aging Infrastructure*, Newport Beach, CA, USA, June. <https://doi.org/10.1117/12.387801>
- Kurata, M., Kim, J., Lynch, J.P., van der Linden, G.W., Sedarat, H., Thometz, E., Hipley, P. and Sheng, L.-H. (2013), “Internet-enabled wireless structural monitoring systems: Development and permanent deployment at the New Carquinez suspension bridge”, *J. Struct. Eng.*, **139**(10), 1688-1702. [https://doi.org/10.1061/\(ASCE\)ST.1943-541X.0000609](https://doi.org/10.1061/(ASCE)ST.1943-541X.0000609)
- Kwon, K. and Frangopol, D.M. (2010), “Bridge fatigue reliability assessment using probability density functions of equivalent stress range based on field monitoring data”, *Int. J. Fatigue*, **32**(8), 1221-1232. <https://doi.org/10.1016/j.ijfatigue.2010.01.002>
- Jin, C., Li, J., Jang, S., Sun, X. and Christenson, R. (2015), “Structural damage detection for in-service highway bridge under operational and environmental variability”, *Proceedings Volume 9435, Sensors and Smart Structures Technologies for Civil, Mechanical, and Aerospace Systems*, San Diego, CA, USA, March.
- Jin, C., Jang, S., Sun, X., Li, J. and Christenson, R. (2016), “Damage detection of a highway bridge under severe temperature changes using extended Kalman filter trained neural network”, *J. Civil Struct. Health Monitor.*, **6**(3), 545-560. <https://doi.org/10.1007/s13349-016-0173-8>
- Jo, H., Sim, S.-H., Nagayama, T. and Spencer Jr., B.F. (2012), “Development and application of high-sensitivity wireless smart sensors for decentralized stochastic modal identification”, *J. Eng. Mech.*, **138**(6), 683-694. [https://doi.org/10.1061/\(ASCE\)EM.1943-7889.0000352](https://doi.org/10.1061/(ASCE)EM.1943-7889.0000352)
- Land, R., Murugesu, G. and Raghavendrachar, M. (2003), “Assessing Bridge Performance-When, What, and How”, Technical Memorandum of Public Works Research Institute.  
<https://www.pwri.go.jp/eng/ujnr/tc/g/pdf/19/7-2land.pdf>
- Lee, L.S.W. (2005), “Monitoring and service life estimation of reinforced concrete bridge decks rehabilitated with externally bonded carbon fiber reinforced polymer (CFRP) composites”, Ph.D. Dissertation; University of California, San Diego, CA, USA.
- Lee, L.S., Karbhari, V.M. and Sikorsky, C. (2007), “Structural health monitoring of CFRP strengthened bridge decks using ambient vibrations”, *Struct. Health Monitor.*, **6**(3), 199-214. <https://doi.org/10.1177/1475921707081109>
- Liang, Y.J. and Chen, W. (2014), “Bridge fatigue life prediction using Mittag-Leffler distribution”, *Fatigue Fract. Eng. Mater. Struct.*, **37**(3), 255-264. <https://doi.org/10.1111/ffe.12110>

- Liu, M., Frangopol, D.M. and Kim, S. (2009), "Bridge system performance assessment from structural health monitoring: A case study", *J. Struct. Eng.*, **135**(6), 733-742.  
[https://doi.org/10.1061/\(ASCE\)ST.1943-541X.0000014](https://doi.org/10.1061/(ASCE)ST.1943-541X.0000014)
- Lobo-Aguilar, S., Zhang, Z., Jiang, Z. and Christenson, R. (2019), "Infrasound-based noncontact sensing for bridge structural health monitoring", *J. Bridge Eng.*, **24**(5), 04019033.  
[https://doi.org/10.1061/\(ASCE\)BE.1943-5592.0001385](https://doi.org/10.1061/(ASCE)BE.1943-5592.0001385)
- Lu, P., Phares, B.M., Greimann, L.F. and Wipf, T.J. (2010), "Bridge structural health monitoring system using statistical control chart analysis", *Transport. Res. Rec.: J. Transport. Res. Board.*, **2172**(1), 123-131.  
<https://doi.org/10.3141/2172-14>
- Luo, L., Feng, M.Q. and Wu, Z.Y. (2018), "Robust vision sensor for multi-point displacement monitoring of bridges in the field", *Eng. Struct.*, **163**, 255-266. <https://doi.org/10.1016/j.engstruct.2018.02.014>
- Maguire, M. (2013), "Transverse and longitudinal bending of segmental concrete box girder bridges", Ph.D. Dissertation; Virginia Tech, Blacksburg, VA, USA.
- Maguire, M., Roberts-Wollmann, C. and Cousins, T. (2018), "Live-load testing and long-term monitoring of the Varina-Enon bridge: investigating thermal distress", *J. Bridge Eng.*, **23**(3), 04018003.  
[https://doi.org/10.1061/\(ASCE\)BE.1943-5592.0001200](https://doi.org/10.1061/(ASCE)BE.1943-5592.0001200)
- Mahmoud, H.N., Connor, R.J. and Bowman, C.A. (2005), "Results of the fatigue evaluation and field monitoring of the I-39 Northbound Bridge over the Wisconsin River", Report No. 05-04; Lehigh University, Bethlehem, PA, USA.
- Mahmoud, H.N., Hodgson, I.C. and Bowman, C.A. (2006), "Instrumentation, Field Testing, and Fatigue Evaluation of Selected Approach Spans of the Throgs Neck Bridge (TN82) over the East River, New York", Report No. 06-17; Lehigh University, Bethlehem, PA, USA.
- McNeil, S., Lee, E., Li, Y., Chiquoine, R., Heaslip, K. and Herning, G. (2019), "COLLABORATIVE PROPOSAL: The Connection between State of Good Repair and Resilience: Measures for Pavements and Bridges", Report No. CAIT-UTC-NC45; Department of Civil and Environmental Engineering, University of Delaware, Newark, DE, USA.
- Mehrabani, A.B. and Farhangdoust, S. (2018), "A laser-based noncontact vibration technique for health monitoring of structural cables: background, success, and new developments", *Adv. Acoust. Vib.*, **2018**.  
<https://doi.org/10.1155/2018/8640674>
- Modares, M. and Waksman, N. (2013), "Overview of structural health monitoring for steel bridges", *Pract. Period. Struct. Des. Constr.*, **18**(3), 187-191. [https://doi.org/10.1061/\(ASCE\)SC.1943-5576.0000154](https://doi.org/10.1061/(ASCE)SC.1943-5576.0000154)
- Moreu, F., Jo, H., Li, J., Kim, R.E., Cho, S., Kimmle, A., Scola, S., Le, H., Spencer Jr, B.F. and LaFave, J.M. (2015), "Dynamic assessment of timber railroad bridges using displacements", *J. Bridge Eng.*, **20**(10), 04014114. [https://doi.org/10.1061/\(ASCE\)BE.1943-5592.0000726](https://doi.org/10.1061/(ASCE)BE.1943-5592.0000726)
- Moreu, F., Li, J., Jo, H., Kim, R.E., Scola, S., Spencer Jr, B.F. and LaFave, J.M. (2016), "Reference-free displacements for condition assessment of timber railroad bridges", *J. Bridge Eng.*, **21**(2), 04015052.  
[https://doi.org/10.1061/\(ASCE\)BE.1943-5592.0000805](https://doi.org/10.1061/(ASCE)BE.1943-5592.0000805)
- Moreu, F., Li, X., Li, S. and Zhang, D. (2018), "Technical specifications of structural health monitoring for highway bridges: new Chinese structural health monitoring code", *Front. Built Environ.*, **4**, p. 10.  
<https://doi.org/10.3389/fbuil.2018.00010>
- Moreno-Gomez, A., Perez-Ramirez, C.A., Dominguez-Gonzalez, A., Valtierra-Rodriguez, M., Chavez-Alegria, O. and Amezcua-Sanchez, J.P. (2018), "Sensors used in structural health monitoring", *Arch. Comput. Methods Eng.*, **25**(4), 901-918. <https://doi.org/10.1007/s11831-017-9217-4>
- Nagarajaiah, S. and Erazo, K. (2016), "Structural monitoring and identification of civil infrastructure in the United States", *Struct. Monit. Maint., Int. J.*, **3**(1), 51-69. <https://doi.org/10.12989/smm.2016.3.1.051>
- Napolitano, R., Liu, Z., Sun, C. and Glisic, B. (2019), "Combination of image-based documentation and augmented reality for structural health monitoring and building pathology", *Front. Built Environ.*, **5**, p. 50.  
<https://doi.org/10.3389/fbuil.2019.00050>
- Natalicchio, C. (2018), "Model calibration of the Indian River Inlet Bridge using structural health monitoring strain data", Ph.D. Dissertation; University of Delaware, Newark, DE, USA.

- Nichols, G. (2017), “Statistical Models of I-15 Bridge C-846: Changes in Natural Frequencies due to Temperature”, Master of Science Thesis; Utah State University, Logan, UT, USA.
- Nichols, G.A., Halling, M.W. and Barr, P.J. (2018), “Installation of Thermocouples, and Analysis of Temperature Data from the 21st South Bridge”, Report No. CAIT-UTC-NC33; Utah State University, Logan, UT, USA.
- Norouzi, M., Zhang, F., Hunt, V. and Helmicki, A.J. (2014), “Structural Health Monitor of the US Grant Bridge (Data Patterns)”, *NDE/NDT for Structural Materials Technology for Highway and Bridges*, Washington, DC, USA, August.
- O’Connor, S.M., Zhang, Y., Lynch, J.P., Ettouney, M.M. and Jansson, P.O. (2017), “Long-term performance assessment of the Telegraph Road Bridge using a permanent wireless monitoring system and automated statistical process control analytics”, *Struct. Infrastruct. Eng.*, **13**(5), 604-624.  
<https://doi.org/10.1080/15732479.2016.1171883>
- Orcesi, A. and Frangopol, D. (2011), “Optimization of Bridge Maintenance Strategies Based on Structural Health Monitoring Information”, *Struct. Saf.*, **33**(1), 26-41. <https://doi.org/10.1016/j.strusafe.2010.05.002>
- Orsak, J. (2019), “A New Method for Detecting the Onset of Scour and Managing Scour Critical Bridges”, Report No. DOT/FRA/ORD-19/32; US Department of Transportation, Federal Railroad Administration.
- Pace, J.M., Barr, P.J., Powelson, P. and Mountain Plains Consortium (2019), Prestress Losses and Development of Short-term Data Acquisition System for Bridge Monitoring (No. MPC-19-387), Mountain Plains Consortium.
- Pakzad, S.N. (2010), “Development and deployment of large scale wireless sensor network on a long-span bridge”, *Smart Struct. Syst., Int. J.*, **6**(5-6), 525-543. [https://doi.org/10.12989/sss.2010.6.5\\_6.525](https://doi.org/10.12989/sss.2010.6.5_6.525)
- Pakzad, S.N. and Fennes, G.L. (2009), “Statistical analysis of vibration modes of a suspension bridge using spatially dense wireless sensor network”, *J. Struct. Eng.*, **135**(7), 863-872.  
[https://doi.org/10.1061/\(ASCE\)ST.1943-541X.0000033](https://doi.org/10.1061/(ASCE)ST.1943-541X.0000033)
- Pakzad, S.N., Fennes, G.L., Kim, S. and Culler, D.E. (2008), “Design and implementation of scalable wireless sensor network for structural monitoring”, *J. Infrastruct. Syst.*, **14**(1), 89-101.  
[https://doi.org/10.1061/\(ASCE\)1076-0342\(2008\)14:1\(89\)](https://doi.org/10.1061/(ASCE)1076-0342(2008)14:1(89))
- Peiris, A., Sun, C. and Harik, I. (2018), “Lessons learned from six different structural health monitoring systems on highway bridges”, *J. Low Freq. Noise, Vib. Act. Control*, **39**(3), 616-630.  
<https://doi.org/10.1177/1461348418815406>
- Phares, B.M., Wipf, T.J., Greimann, L.F., Wood, D.L., Lee, Y.S. and Doornink, J.D. (2007), “Evaluation of steel bridges (volume II): structural health monitoring system for secondary road bridges”, Report No. IHRB Project TR-493; Center for Transportation Research and Education, Iowa State University, Ames, IA, USA.
- Pines, D. and Aktan, A.E. (2002), “Status of structural health monitoring of long-span bridges in the United States”, *Prog. Struct. Eng. Mater.*, **4**(4), 372-380. <https://doi.org/10.1002/pse.129>
- Pure Technologies (2020), <https://puretechltd.com/case-studies/texas-dept-transportation-fred-hartman-bridge/>
- Robertson, I.N. (2005), “Prediction of vertical deflections for a long-span prestressed concrete bridge structure”, *Eng. Struct.*, **27**(12), 1820-1827. <https://doi.org/10.1016/j.engstruct.2005.05.013>
- Sanayei, M., Phelps, J.E., Sipple, J.D., Bell, E.S. and Brenner, B.R. (2012), “Instrumentation, nondestructive testing, and finite-element model updating for bridge evaluation using strain measurements”, *J. Bridge Eng.*, **17**(1), 130-138. [https://doi.org/10.1061/\(ASCE\)BE.1943-5592.0000228](https://doi.org/10.1061/(ASCE)BE.1943-5592.0000228)
- Santini Bell, E., Sipple, J.D., Lefebvre, P., Phelps, J., Brenner, B. and Sanayei, M. (2010), “Instrumentation, Modeling, and Monitoring of a Concrete Bridge from Construction Through Service”, *Transportation Research Board 89th Annual Meeting*, Washington, DC, USA, January.
- Santini Bell, E., Lefebvre, P.J., Sanayei, M., Brenner, B., Sipple, J.D. and Peddle, J. (2013), “Objective load rating of a steel-girder bridge using structural modeling and health monitoring”, *J. Struct. Eng.*, **139**(10), 1771-1779. [https://doi.org/10.1061/\(ASCE\)ST.1943-541X.0000599](https://doi.org/10.1061/(ASCE)ST.1943-541X.0000599)
- Schenewerk, M.S., Harris, R.S. and Stowell, J. (2006), “Structural health monitoring using GPS”, *Bridges*, **9**(2), 01036035.
- Schultz, A.E., Morton, D.L., Tillmann, A.S., Campos, J.E., Thompson, D.J., Lee-Norris, A.J. and Ballard,

- R.M. (2014), “Acoustic Emission Monitoring of a Fracture-Critical Bridge”, Report No. MN/RC 2014-15; University of Minnesota, Minneapolis, MN, USA.
- Sen, D., Erazo, K., Zhang, W., Nagarajaiah, S. and Sun, L. (2019), “On the effectiveness of principal component analysis for decoupling structural damage and environmental effects in bridge structures”, *J. Sound Vib.*, **457**, 280-298. <https://doi.org/10.1016/j.jsv.2019.06.003>
- Seo, J., Phares, B., Lu, P., Wipf, T. and Dahlberg, J. (2013), “Bridge rating protocol using ambient trucks through structural health monitoring system”, *Eng. Struct.*, **46**, 569-580. <https://doi.org/10.1016/j.engstruct.2012.08.012>
- Shahsavari, V., Mashayekhizadeh, M., Mehrkash, M. and Santini-Bell, E. (2019), “Diagnostic testing of a vertical lift truss bridge for model verification and decision-making support”, *Front. Built Environ.*, **5**, p. 92. <https://doi.org/10.3389/fbuil.2019.00092>
- Shahsavari, V., Mehrkash, M. and Santini-Bell, E. (2020), “Damage detection and decreased load-carrying capacity assessment of a vertical-lift steel truss bridge”, *J. Perform. Constr. Facil.*, **34**(2), 04019123. [https://doi.org/10.1061/\(ASCE\)CF.19r43-5509.0001400](https://doi.org/10.1061/(ASCE)CF.19r43-5509.0001400)
- Sharyatpanahi, S.B.G. (2015), “Structural health monitoring of bridges using wireless sensor networks” Master of Science Thesis; New Jersey Institute of Technology, Newark, NJ, USA. <https://digitalcommons.njit.edu/theses/231/>
- Shenton III, H.W., Chajes, M.J., Wenczel, G. and Cardinal, J. (2013), “Inaugural Load Test of the Charles W. Cullen Bridge at Indian River Inlet”, Report No. DCT 238; Center for Innovative Bridge Engineering, University of Delaware, Newark, DE, USA.
- Shenton III, H.W., Chajes, M.J., Wenczel, G. and Al-Khateeb, H.T. (2016), “Load Tests of the Charles W. Cullen Bridge at Indian River Inlet”, Technical Report; Center for Innovative Bridge Engineering, University of Delaware, Newark, DE, USA.
- Shenton III, H.W., Al-Khateeb, H.T., Chajes, M.J. and Wenczel, G. (2017), “Indian river inlet bridge (part A): Description of the bridge and the structural health monitoring system”, *Bridge Struct.*, **13**(1), 3-13.
- SMARTEC (2017a), New Mexico I10 Bridge, <https://smartec.ch/en/case-study/new-mexico-i10-bridge/>, Published on January 30<sup>th</sup>, 2017. Last date accessed May 19, 2020.
- SMARTEC (2017b), Rio Puerco, <https://smartec.ch/en/case-study/rio-puerco/>. Published on January 31<sup>st</sup>, 2017. Last date accessed May 19, 2020.
- Soltész, S. (2002), “Strain monitoring for Horsetail Falls and Sylvan Bridges”, Report No. FHWA-OR-DF-02-17; Department of Transportation, OR, USA.
- Sun, L., Shang, Z., Xia, Y., Bhowmick, S. and Nagarajaiah, S. (2020), “Review of bridge structural health monitoring aided by big data and artificial intelligence: from condition assessment to damage detection”, *J. Struct. Eng.*, **146**(5), 04020073. [https://doi.org/10.1061/\(ASCE\)ST.1943-541X.0002535](https://doi.org/10.1061/(ASCE)ST.1943-541X.0002535)
- Swartz, R., Lynch, J., Sweetman, B. and Rolfes, R. (2010), “Structural monitoring of wind turbines using wireless sensor networks”, *Smart Struct. Syst., Int. J.*, **6**(3), 183-196. <https://doi.org/10.12989/sss.2010.6.3.183>
- Taheri, S. (2019), “A review on five key sensors for monitoring of concrete structures”, *Constr. Build. Mater.*, **204**, 492-509. <https://doi.org/10.1016/j.conbuildmat.2019.01.172>
- Talebinejad, I., Fischer, C. and Ansari, F. (2011), “Numerical evaluation of vibration-based methods for damage assessment of cable-stayed bridges”, *Comput.-Aided Civil Infrastruct. Eng.*, **26**(3), 239-251. <https://doi.org/10.1111/j.1467-8667.2010.00684.x>
- Texas Department of Transportation (2020), <https://puretechltd.com/case-studies/texas-dept-transportation-fred-hartman-bridge/>
- Torbol, M., Kim, S. and Chou, P.H. (2013), “Remote structural health monitoring systems for next generation SCADA”, *Smart Struct. Syst., Int. J.*, **11**(5), 511-531. <https://doi.org/10.12989/sss.2013.11.5.511>
- Virginia Department of Transportation (2019), [https://www.virginiadot.org/info/resources/bridge\\_defs.pdf](https://www.virginiadot.org/info/resources/bridge_defs.pdf)
- Watkins, S.E., Fonda, J.W. and Nanni, A. (2007), “Assessment of an instrumented reinforced-concrete bridge with fiber-reinforced-polymer strengthening”, *Opt. Eng.*, **46**(5), 051010. <https://doi.org/10.1117/1.2740758>

- Weinmann, T.L. (2015), "Huey P. Long Bridge Widening and Truss Lift Monitoring", In: *Structures Congress 2015*, Portland, OR, USA, April.
- Whelan, M.J., Gangone, M.V., Janoyan, K.D. and Jha, R. (2009), "Real-time wireless vibration monitoring for operational modal analysis of an integral abutment highway bridge", *Eng. Struct.*, **31**(10), 2224-2235. <https://doi.org/10.1016/j.engstruct.2009.03.022>
- Wipf, T.J., Phares, B.M., Greimann, L.F., Wood, D.L. and Doornink, J.D. (2007), "Evaluation of steel bridges (Volume I): monitoring the structural condition of fracture-critical bridges using fiber optic technology", Report No. IHRB Project TR-493; Center for Transportation Research and Education, Iowa State University, Ames, IA, USA.
- Worden, K., Farrar, C.R., Manson, G. and Park, G. (2007), "The fundamental axioms of structural health monitoring", *Proc. R. Soc. A*, **463**, 1639-1664. <https://doi.org/10.1098/rspa.2007.1834>
- Wu, Z.Y., Zhou, K., Shenton, H.W. and Chajes, M.J. (2019), "Development of sensor placement optimization tool and application to large-span cable-stayed bridge", *J. Civil Struct. Health Monitor.*, **9**(1), 77-90. <https://doi.org/10.1007/s13349-018-0320-5>
- Xiao, F., Hulsey, J.L. and Balasubramanian, R. (2017), "Fiber optic health monitoring and temperature behavior of bridge in cold region", *Struct. Control Health Monitor.*, **24**(11). <https://doi.org/10.1002/stc.2020>
- Xiao, P., Wu, Z.Y., Christenson, R. and Lobo-Aguilar, S. (2020), "Development of video analytics with template matching methods for using camera as sensor and application to highway bridge structural health monitoring", *J. Civil Struct. Health Monit.*, **10**, 405-424. <https://doi.org/10.1007/s13349-020-00392-6>
- Xu, Y. and Xia, Y. (2011), *Structural Health Monitoring of Long-Span Suspension Bridges*, CRC Press, Boca Raton, FL, USA.
- Yan, R., Chen, X. and Mukhopadhyay, S.C. (2017), *Structural Health Monitoring*, Springer, Berlin, Germany.
- Yarnold, M.T. and Moon, F.L. (2015), "Temperature-based structural health monitoring baseline for long-span bridges", *Eng. Struct.*, **86**, 157-167. <https://doi.org/10.1016/j.engstruct.2014.12.042>
- Yarnold, M.T., Moon, F.L., Aktan, A.E. and Glisic, B. (2012a), "Structural monitoring of the Tacony-Palmyra Bridge using video and sensor integration for enhanced data interpretation", *Proceedings of the 6th International Conference on Bridge Maintenance, Safety and Management*, Stresa, Lake Maggiore, Italy, July.
- Yarnold, M.T., Moon, F.L., Dubbs, N.C. and Aktan, A.E. (2012b), "Evaluation of a long-span steel tied arch bridge using temperature-based structural identification", *Proceedings of the 6th International Conference on Bridge Maintenance, Safety and Management*, Stresa, Lake Maggiore, Italy, July.
- Yun, H., Nayeri, R., Tasbihgoo, F., Wahbeh, M., Caffrey, J., Wolfe, R., Nigbor, R., Masri, S.F., Abdel-Ghaffar, A. and Sheng, L.-H. (2008), "Monitoring the collision of a cargo ship with the Vincent Thomas Bridge", *Struct. Control Health Monitor.*, **15**(2), 183-206. <https://doi.org/10.1002/stc.213>
- Zhang, Y., Kurata, M. and Lynch, J.P. (2017), "Long-term modal analysis of wireless structural monitoring data from a suspension bridge under varying environmental and operational conditions: System design and automated modal analysis", *J. Eng. Mech.*, **143**(4), 04016124. [https://doi.org/10.1061/\(ASCE\)EM.1943-7889.0001198](https://doi.org/10.1061/(ASCE)EM.1943-7889.0001198)
- Zhu, Z., Davidson, M.T., Harik, I.E. and Sun, C. (2015), "Effect Of Thermal Loads on Substructures: New Trammel Creek Bridge on KY-100 In Allen Co., Kentucky", Report No. KTC-15-14/SPR10-408-1F; Kentucky Transportation Center, College of Engineering, University of Kentucky, Frankfort, KY, USA.
- Zuo, D. and Jones, N. (2005), Stay-cable vibration monitoring of the Fred Hartman Bridge (Houston, Texas) and the Veterans Memorial Bridge (Port Arthur, Texas), FHWA/TX-06/0-1401-2 Report.
- Zuo, D. and Jones, N.P. (2010), "Interpretation of field observations of wind-and rain-wind-induced stay cable vibrations", *J. Wind Eng. Indust. Aerodyn.*, **98**(2), 73-87. <https://doi.org/10.1016/j.jweia.2009.09.004>